Inulin reduces *Ralstonia* invasion by promoting cooperation between *Lysinibacillus sphaericus* and *Pseudarthrobacter* spp.

Tao Yan[1, #], Ying Guan[1, #], Xinlan Mei[1], Ziru Zhang[1], Tianxiang Zhu[1], Yang Gao[1], Xiaofang Wang[1], Yangchun Xu[1], Qirong Shen[1], Zhong Wei[1], Tianjie Yang[1, *]

[1] Jiangsu Provincial Key Lab of Solid Organic Waste Utilization, Jiangsu Collaborative Innovation Center of Solid Organic Wastes, Educational Ministry Engineering Center of Resource-saving fertilizers, Nanjing Agricultural University, Nanjing, Jiangsu 211800, China

* Correspondence: tjyang@njau.edu.cn

# These authors contributed equally

Abstract

In field production, beneficial microbial agents are typically applied along with key resources that beneficial microbes prefer to utilize. This practice aims to help the beneficial microbes colonize the field and exert their disease resistance functions. However, the mechanisms by which these key resources influence the colonization and disease resistance effects of beneficial microbes remain unknown. In this study, we found that inulin can enhance the growth capacity of *Lysinibacillus sphaericus* HR92 and its ability to inhibit *Ralstonia solanacearum*. Further investigation revealed that inulin can enhance strain HR92's flagellar assembly, bacterial chemotaxis, fatty acid metabolism, and siderophore synthesis capabilities, ultimately improving strain HR92's effectiveness in controlling bacterial wilt. Moreover, adding inulin to the soil can enrich *Pseudarthrobacter* strains. This genus enhances the expression of genes involved in the synthesis of the antibacterial substance HR92, and competes for nutrients with *Ralstonia solanacearum*, thereby further inhibiting the occurrence of bacterial wilt disease. Additionally, the combination of inulin and *Pseudarthrobacter* strains upregulates the valine and leucine pathway genes in strain HR92. These genes play a crucial role in the synthesis of surfactin and the antimicrobial VOC 3-methyl-1-butanol. We have demonstrated that the addition of key resources not

only enhances the control efficacy of beneficial bacteria against soil-borne diseases but also enriches the “helpers” of beneficial bacteria in soil.

Importance

Ralstonia solanacearum is a plant pathogen that can cause bacterial wilt in several important crops. Given the limitations of beneficial bacterial inoculation, we propose a strategy to enhance the biocontrol efficacy of beneficial microorganisms by utilizing key resources. In this study, we demonstrate that key resources inulin can improve the biological control effects of beneficial bacteria, thereby maintaining plant health. Furthermore, we found that increasing the concentration of inulin altered the diversity of the rhizosphere microbiota and specifically enriched the abundance of *Pseudarthrobacter*, which compete with pathogens for nutrients on one hand and, on the other hand, synergize with inulin to enhance the biocontrol efficacy of the beneficial bacterium HR92. Together, our study reveals that key resources can enhance the biocontrol efficacy of beneficial bacteria and enrich potential beneficial bacteria in resident microbial communities, further reducing tomato diseases.

Keywords: Tomato bacterial wilt, *Ralstonia solanacearum*, rhizosphere, inulin, *Lysinibacillus sphaericus*

Introduction

Soil-borne plant pathogens cause major economic losses to agricultural production due to lack of efficient control methods (1–5). In recent years, researchers have increasingly explored the use of biological control methods, which are ecologically friendly and exhibit specificity in pathogen suppression (6–9). Beneficial microbes can prevent pathogenic invasion of plant root systems through various mechanisms, they can secrete antagonistic substances that directly inhibit the growth of pathogens or their "helpers" (10), preventing colonization or invasion of plant roots. Some beneficial bacteria compete with pathogens for rhizosphere resources, thereby suppressing pathogen growth through nutrient competition. Moreover, introduced beneficial microbes can stimulate soil native resident microbiomes (11), engaging in metabolic interactions that fortify the rhizosphere, creating a more resilient barrier that pathogens find difficult to breach (10, 12–15). Studies have shown that *Lysinibacillus sphaericus* is an effective biocontrol agent against bacterial wilt in tomatoes (16–19). Specifically, *L. sphaericus* inhibits the growth of *R. solanacearum* through the secretion of volatile organic compounds (VOCs) such as dicarboxylic esters and 3-methyl-1-butanol (20), as well as cyclic lipopeptides like surfactin and bacitracin (21–23).

Due to the limited availability of nutrients in the rhizosphere and the complex conditions of the field environment (24, 25), the inoculated beneficial bacteria often lack a competitive edge over soil native resident microbiomes, preventing them from efficiently colonizing the rhizosphere and exhibiting their disease-suppressive functions (26–28). Recent studies have proposed providing nutritional carriers for inoculated beneficial bacteria to enhance their biocontrol efficacy in the rhizosphere (29–34). For instance, adding organic fertilizers, biochar, or amino acid-based fertilizers along with the beneficial microbes has been shown to improve their survival in the rhizosphere. However, these organic carriers are generally utilized by a wide range of soil microorganisms, lacking specificity, and cannot be exclusively exploited by beneficial bacteria. In recent years, research in the field of gut

microbiota has suggested adding resources preferentially utilized by beneficial bacteria along with their introduction to target and enhance their colonization in the gut (35, 36). Due to the analogous roles of the rhizosphere and the gut in host immunity and ecological function, we hypothesize that the application of targeted resources capable of selectively enhancing the colonization efficiency of beneficial bacteria in the rhizosphere will promote their stable establishment in the root environment (37–39), ultimately improving their biocontrol performance. Soil microorganisms in the rhizosphere are often strongly influenced by plant root exudates, with sugars in these exudates playing a crucial role in recruiting beneficial bacteria and maintaining plant health (40–42). Thus, we focused on soluble sugars from root exudates to identify a compound capable of selectively enhancing the colonization capacity of *Lysinibacillus sphaericus*. Through this approach, we aim to explore how such a resource influences the biocontrol potential of beneficial bacteria within the complex rhizosphere environment.

Unlocking the potential of specific resources to enhance the targeted colonization of beneficial bacteria in the rhizosphere, while understanding their effects on soil native microbial communities, is crucial for managing soil-borne diseases in agricultural production. We utilized *L. sphaericus* HR92 along with inulin, which has been shown to boost both the growth and antibacterial activity of strain HR92. By inoculating the beneficial bacteria and varying concentrations of inulin to the tomato roots, we observed the colonization potential of strain HR92 and its impact on the assembly of bacterial communities in the tomato rhizosphere. Our findings reveal that inulin not only directly enhances strain HR92 colonization and disease suppression capabilities but also enriches specific soil native resident microbiomes. These native microbes, on one hand, exhibit inhibitory effects on pathogens and, on the other, enhance the disease resistance of beneficial bacteria. Finally, we used transcriptomics to determine the influence of inulin and native soil microbes on strain HR92.

104 ## Materials and methods

105 ### Strains and growth conditions

106 The plant pathogen used in this study was *Ralstonia solanacearum* QL-Rs1115
107 (GenBank: GU390462) (43), and the beneficial bacterium was *Lysinibacillus*
108 *sphaericus* HR92 (GenBank: JF700465.1) (19). The strain was routinely grown in
109 nutrient broth medium at 30 °C with shaking at 170 rpm in NB medium (nutrient
110 broth, 10.0 g glucose L^{-1}; 5.0 g peptone L^{-1}, 0.5 g yeast extract L^{-1}, and 3.0 g beef
111 extract L^{-1}, pH 7.0).

112 In *vitro* co-culture experiments, we used strain *R. solanacearum* QL-RFP, that
113 QL-Rs1115 was tagged with the stable pYC12-mCherry plasmid (excitation
114 wavelength: 587 nm, absorption wavelength: 610 nm) (14). The tagged plasmid had
115 no significant impact on growth and virulence of the pathogen *R. solanacearum* (14).
116 The strain *L. sphaericus* HR92 carries green fluorescence plasmid (excitation
117 wavelength: 488 nm, absorption wavelength: 510 nm). The pathogen cells were
118 harvested by centrifugation (6000 rpm, 10 min), washed twice with sterile saline
119 solution (0.9% NaCl), and diluted to a density of 10^8 colony-forming units (CFU)
120 ml^{-1} based on the optical density 600 (OD_{600} = 0.5) before all the experiments.

121 ### Effects of various sugars on the growth of *Ralstonia solanacearum* and HR92

122 The bacterial strain HR92, and *R. solanacearum* QL-Rs1115 were grown overnight in
123 NB medium at 30 °C with shaking at 170 rpm. Cells were washed three times with
124 0.85% NaCl and resuspended to an OD_{600} of 0.5 (approximate 10^7 CFU mL^{-1}). Bacteria
125 was cultured in a 96-well microtiter plate. Each well contained a total of 200 µL
126 culture liquid: 178 µL NB medium, 20 µL of 1mM sugars solution (final concentration
127 0.1mM), and 2 µL bacterial suspension. We set treatment without sugars (the same
128 volume sterile water instead) as control. The microtiter plate was incubated at 30 °C
129 with agitation of 170 rpm. Bacterial growth (OD_{600}) was measured after 48 h by
130 using a SpectraMax M5 spectrophotometer (Molecular Devices, Sunnyvale, CA, USA).
131 All treatments were performed with three replicates.

132 ### Effect of various sugars on the ability of strain HR92 to inhibit *R. solanacearum*

133 We selected sugars that did not directly promote the growth of *R. solanacearum* for
134 subsequent experiments. The bacterial strains HR92 and R. solanacearum QL-RFP
135 were grown overnight in NB medium at 30 °C with shaking at 170 rpm. Cells were
136 washed three times with 0.85% NaCl and resuspended to an OD600 of 0.5
137 (approximately 10^7 CFU mL^{-1}). The bacteria were cultured in 96-well microtiter
138 plates. Each well contained a total of 200 µL of culture: 176 µL NB medium, 20 µL
139 of 1 mM sugar solution (final concentration 0.1 mM), and 2 µL each of HR92 and
140 QL-RFP. We set treatment without sugars (the same volume sterile water instead) as
141 control. The microtiter plates were incubated at 30 °C with shaking at 170 rpm.
142 Bacterial growth (OD_{600}) was measured after 48 hours using a SpectraMax M5
143 spectrophotometer (Molecular Devices, Sunnyvale, CA, USA). In addition, red
144 fluorescence of QL-RFP (excitation wavelength: 587 nm; emission wavelength:
145 610 nm) was measured, and the biomass of *R. solanacearum* under co-culture with
146 HR92 and sugars was calculated using log (RFU/OD_{600}). All treatments were
147 performed with three replicates.

148 **Greenhouse experiment setup and sample collection**

149 Surface-sterilized tomato seeds (*Solanum lycopersicum,* cultivar "Hong'ai") were
150 germinated on water-agar plates for 3 days before sowing into 72-well trays filled
151 with growth substrate (50 g substrate per well; commercially available from
152 Jiangsu-Xingnong Substrate Technology Co., Ltd). At the three-leaf stage (17 days
153 after sowing), a subset of tomato plants of similar size was selected and transplanted
154 into seedling cups containing natural soil (200 g per cell). Seedlings were grown
155 under controlled greenhouse conditions (25-30 °C, 16/8 h day/night cycle, 200 µmol
156 m^{-2} s^{-1} light density, and 70% relative humidity).

157 **Part1: Inulin enhances the disease-suppressive effect of HR92**

158 Seven days after transplantation, strain HR92 and inulin were inoculated together
159 into the rhizosphere soil of each plant. The final density of strain HR92 was 10^8 CFU
160 g^{-1} soil. The final concentration of inulin was adjusted according to each treatment.
161 Seven days after co-inoculation of strain HR92 and inulin, the pathogen *R.*
162 *solanacearum* QL-Rs1115 was inoculated into the rhizosphere soil of each plant at a

163 final density of 10^6 CFU g^{-1} soil. The greenhouse experiment comprised four
164 treatments, including only pathogen, only HR92, HR92 with 0.1% inulin (1 g kg^{-1} soil),
165 and HR92 with 0.3% inulin (3 g kg^{-1} soil) (Fig. S1). Each treatment had four biological
166 replicates, with each replicate consisting of five individual tomato plants, resulting in
167 a total of 80 plants (20 plants per treatment x 4 treatments). Tomato plants regularly
168 watered with sterile water, and their positions were randomized every two days.
169 Seven days after inoculation with *R. solanacearum*, the tomato plants began to
170 exhibit disease symptoms. Disease index was recorded seven days after
171 transplantation on a scale of 0 to 4 (0, no signs of wilting; 1, 1%–25% lead area wilted;
172 2, 26%–50% leaf area wilted; 3, 51%–75% leaf area wilted; and 4, 76%–100% leaf
173 area wilted), and was calculated using the formula: DS = ∑ (number of diseased
174 plants with given index × DI)/ (total number of plants infected × highest DI) (44). Soil
175 samples from the rhizosphere of both healthy and diseased plants were collected
176 and stored at -80 ℃.

177 **Part II: P265, P397, and inulin enhance the disease-suppressive effect of HR92.**

178 In a separate set of experiments with a similar design, we further evaluated the
179 effects of two key bacterial strains (P265 and P397) in enhancing the biocontrol
180 effect of HR92. Seven days after transplantation, strains P265, P397, and HR92 were
181 co-inoculated into the rhizosphere together with inulin. The total bacterial density
182 was adjusted to 10^8 CFU g^{-1} soil. Seven days after this co-inoculation, *R.*
183 *solanacearum* QL-Rs1115 was introduced at 10^6 CFU g^{-1} soil. Treatments and
184 replication were conducted as in Part I, with appropriate controls included for
185 comparison. Each treatment had four biological replicates, with each replicate
186 consisting of five individual tomato plants, resulting in a total of 140 plants (20 plants
187 per treatment x 7 treatments).

188 **DNA extraction and 16S rRNA gene amplicon sequencing**

189 Genomic DNA was extracted from 0.5 g of soil using the PowerSoil® DNA Isolation Kit
190 (MoBio, Carlsbad, CA, USA) following the manufacturer's instructions. The purity and
191 concentration of DNA were determined using a NanoDrop ND-1000
192 spectrophotometer (Thermo Fisher Scientific, Carlsbad, CA, USA) and a Qubit 2.0

193 fluorometer (Thermo Fisher Scientific). The V4 region of the bacterial 16S rRNA gene
194 was amplified with primers 563F and 802R (Table S3) (45). A two-step dual indexing
195 strategy for Illumina MiSeq (Illumina, San Diego, CA, USA) sequencing was employed.
196 The PCR thermocycler program included an initial denaturation temperature of 95 ℃
197 for 2 min, then 25 cycles of 95 ℃ for 30 s, 55 ℃ for 30 s, and 72 ℃ for 30 s, and a
198 final elongation step of 72 ℃ for 5 min. The PCR amplification was confirmed by gel
199 electrophoresis on 2% agarose gels. PCR products were purified using AxyPrep PCR
200 Clean-up Kit (Axygen Biosciences, CA, USA). The following library construction and
201 Illumina MiSeq sequencing (2 × 300 bp) were performed by Shanghai Biozeron
202 Biological Technology (Shanghai, China).
203 Raw amplicon reads were processed using the DADA2 pipeline v.1.14.1 (46). In brief,
204 reads were quality checked and primers were removed using trimLeft in the filter
205 AndTrim function. According to the sequence quality, the 16S rRNA gene reads were
206 filtered using default parameters (confidence level at 80%). Chimeras were removed
207 after merging denoised pair-end sequences. Each unique amplicon sequence variant
208 (ASV) was assigned to taxa according to SILVA database v.138.1 (47) for the 16S rRNA
209 gene. For bacteria, non-bacterial ASVs including chloroplasts and mitochondrial reads
210 were removed.
211 **Real-time quantitative PCR analysis**
212 Quantification of strain HR92 (19) and *R. solanacearum* (48) was performed by qPCR
213 using the qTOWER Real-Time PCR system (Analytik jena, Jena, Germany). The specific
214 primers utilized are listed in Table S3. Twenty-microliter reactions were containing 10
215 μL of 2X TB Green Premix Ex Taq (TaKaRa, Beijing, China), 2 μL of DNA, 0.8 μL of each
216 primer (10 μM), 0.4 μL of ROX Reference Dye (TaKaRa, Beijing, China) and 6 μL of
217 Nuclease-free water. Thermal cycling conditions were as follows: 95 ℃ for 3 min,
218 followed by 40 cycles of 95 ℃ for 30 s, 50 ℃ for 30 s, and 72 ℃ for 30 s. Standard
219 curves were used to calculate the gene copy numbers of the target group for each
220 reaction. Each sample was run in triplicate, and results were expressed as log10
221 values of the gene copy numbers per gram of soil.
222 **Screening of Key bacteria**

223 Bacteria were isolated from the rhizosphere of five healthy tomato plants co-treated
224 with HR92 and inulin. Soil samples (1 g) were suspended in sterile water, vortexed,
225 and serially diluted before plating. One hundred microliters of serial dilutions
226 (10^{-4}-10^{-7}) were plated onto 1/3 TSA plates (Tryptic Soy Agar, tryptone 5 g L^{-1}, soy
227 peptone 1.65 g L^{-1}, NaCl 1.65 g L^{-1} and agar 15 g L^{-1}). Plates were incubated at 28 °C
228 until single colonies existed on the medium.
229 All bacterial isolates were identified based on 16S rRNA gene sequence using
230 universal primers 27F and 1492R (Table S3) (49). PCR products were sequenced by
231 Sangon Biotech (Shanghai Co., Ltd, China). 16S rRNA gene sequencing results were
232 blasted against the NCBI database for homologous sequences.
233 **Effect of inulin on bacterial growth**
234 The bacterial strain HR92, P265 (*Pseudarthrobacter siccitolerans*), and P397
235 (*Pseudarthrobacter oxydans*), and *R. solanacearum* QL-Rs1115 were grown overnight
236 in NB medium at 30 °C with shaking at 170 rpm. Cells were washed three times with
237 0.85% NaCl and resuspended to an OD_{600} of 0.5 (approximate 10^7 CFU mL^{-1}). Bacteria
238 was cultured in a 96-well microtiter plate. Each well contained a total of 200 µL
239 culture liquid: 178 µL NB medium, 20 µL 3% inulin (final concentration 0.3%), and 2
240 µL bacterial suspension. We set treatment without inulin (the same volume sterile
241 water instead) as control. The microtiter plate was incubated at 30 °C with agitation
242 of 170 rpm. Bacterial growth (OD_{600}) was measured after 48 h by using a SpectraMax
243 M5 spectrophotometer (Molecular Devices, Sunnyvale, CA, USA). All treatments
244 were performed with four replicates.
245 **Effects of supernatants from HR92, P265, or P397 on *R. solanacearum* growth**
246 **induced by inulin**
247 After measuring bacterial growth, we obtained bacterial supernatant induced by
248 inulin (**supernatant a**) by centrifuging bacterial suspension at 3000 rpm for 15 min
249 with a 96-well filter membrane plate. 2 µL of *R. solanacearum* QL-Rs1115 suspension
250 (OD_{600} = 0.5) were added to a 96-well microtiter plate with each well containing 178
251 µl of NB medium and 20 µl of **supernatant a**. We set a treatment without
252 supernatant (replaced with the same volume of sterile water) as the control. The

253 plate was incubated at 30 °C with agitation of 170 rpm. Ralstonia growth (OD_{600}) was
254 measured after 48 h by using a SpectraMax M5 spectrophotometer (Molecular
255 Devices, Sunnyvale, CA, USA). All treatments were performed with five replicates.

256 **Effect of inulin on the ability of strain HR92, P265, or P397 to inhibit *R.***
257 ***solanacearum* under co-culture conditions**

258 The bacterial strain HR92, P265, P397 and *R. solanacearum* QL-RFP were grown
259 overnight in NB medium at 30 °C with shaking at 170 rpm. Cells were washed three
260 times with 0.85% NaCl and resuspended to an OD_{600} of 0.5 (approximate 10^7 CFU
261 mL^{-1}). Bacteria was cultured in a 96-well microtiter plate. Each well contained a total
262 of 200 µL culture liquid: 176 µL NB medium, 20 µL 3% inulin (final concentration
263 0.3%), 2 µL QL-RFP, and 2 µL of one of the following strains: P265, P397, or HR92. We
264 set treatment without strain and inulin (the same volume sterile water instead) as
265 control. The microtiter plate was incubated at 30 °C with agitation of 170 rpm.
266 Bacterial growth (OD_{600}) was measured after 48 h by using a SpectraMax M5
267 spectrophotometer (Molecular Devices, Sunnyvale, CA, USA). In addition, red
268 fluorescence of QL-RFP (excitation wavelength: 587 nm; emission wavelength:
269 610 nm) was measured, and the biomass of *R. solanacearum* under co-culture with
270 HR92 and sugars was calculated using log(RFU/OD_{600}). All treatments were
271 performed with four replicates.

272 **Carbon resource utilization patterns of the bacterial isolates**

273 The resource utilization patterns of QL-RS1115, HR92, P265 or P397 were assessed
274 across 74 distinct carbon resources (Table S2), including amino acids, organic acids,
275 and sugars commonly found in tomato root exudates. The bacterial strains were
276 grown overnight in NB medium at 30 °C with shaking at 170 rpm. Cells were washed
277 three times with 0.85% NaCl and resuspended to an OD_{600} of 0.5 (approximate 10^7
278 CFU mL^{-1}). Then, 5 µL of each strain was added to a 384-well microtiter plate
279 containing 40 µL of OS minimal medium (50) supplemented with 5 µL of 1 mM of
280 different carbon sources (14). Plates were incubated at 30 °C with agitation at 170
281 rpm, and bacteria growth was measured after 48 h using a SpectraMax M5
282 spectrophotometer (Molecular Devices, Sunnyvale, CA, USA). We set treatment

283 without carbon resource (the same volume sterile water instead) as control. T-tests
284 were conducted to compare the biomass of bacteria under each resource condition
285 with the biomass under the control condition. A significance level of $p < 0.05$
286 indicates that the bacteria can utilize the respective resource. Utilization efficiency
287 was calculated using the formula: (biomass under resource condition - control)/
288 control x 100. Utilization efficiency was categorized into different levels: below 20%
289 was marked as *, 20%-40% as **, 40%-60% as ***, and above 60% as ****. All
290 treatments were performed with four replicates.

291 **Effects of *Pseudarthrobacter* and HR92 combination on *R. solanacearum* growth**
292 **induced by inulin**

293 Strains HR92, P265, P397, and *Ralstonia solanacearum* QL-Rs1115 were grown
294 overnight in NB medium at 30°C with shaking at 170 rpm. After incubation, the cells
295 were washed three times with 0.85% NaCl and resuspended to an OD600 of 0.5
296 (approximately 10^7 CFU/mL). The bacteria were inoculated into a 96-well microtiter
297 plate, with each well containing a total volume of 200 µL: 176 µL NB medium, 20 µL 3%
298 inulin (final concentration 0.3%), and 2 µL of HR92, P265, or P397 suspension. Wells
299 without P265 or P397 (replaced with the same volume of sterile water) were used as
300 controls. The microtiter plate was incubated at 30°C with shaking at 170 rpm for 48
301 hours. After incubation, the bacterial suspension was centrifuged at 3000 rpm for 15
302 minutes using a 96-well filter membrane plate to obtain the bacterial supernatant
303 (**supernatant b**).Then, 2 µL of *R. solanacearum* QL-Rs1115 suspension (OD600 = 0.5)
304 was added to each well of a new 96-well microtiter plate containing 178 µL of NB
305 medium and 20 µL of **supernatant b**. Wells without P265 or P397 (replaced with the
306 same volume of sterile water, only HR92 was included) were used as controls for
307 **supernatant b**. The plate was incubated at 30°C with shaking at 170 rpm. After 48
308 hours, the growth of *R. solanacearum* (OD600) was measured using a SpectraMax
309 M5 spectrophotometer (Molecular Devices, Sunnyvale, CA, USA). All treatments
310 were performed with four replicates.

311 **Effect of *Pseudarthrobacter* spp. on the ability of strain HR92 to inhibit *R.***
312 ***solanacearum***

313 This experiment followed a three-step workflow that was similar to previous
314 inhibition assays. Initially, 2 μL of bacterial suspension (OD_{600} = 0.5) of strain P265 or
315 P397 were incubated in 198 μL of NB medium at 30 °C with agitation at 170 rpm for
316 48 h. The resulting bacterial suspension was transferred to a 96-well filter membrane
317 plate and centrifuged at 3000 rpm for 15 min to collect the supernatant (**supernatant**
318 **c-1**). Next, 2 μL of bacterial suspension (OD_{600} = 0.5) of strain HR92 was incubated
319 with 178 μL of NB medium and 20 μL of **supernatant c-1** under same conditions for
320 48 h. The bacterial suspension was then centrifuged, and the supernatant
321 (**supernatant c-2**) was collected. Finally, 2 μL of *R. solanacearum* suspension (OD_{600} =
322 0.5) was incubated with 178 μL of NB medium and 20 μL of **supernatant c-2** at 30 °C
323 with agitation at 170 rpm for 48 h. We set treatment without **supernatant c-2** (the
324 same volume sterile water instead) as control. Bacterial growth (OD_{600}) was
325 measured using a SpectraMax M5 spectrophotometer (Molecular Devices, Sunnyvale,
326 CA, USA). The effect of *Pseudarthrobacter* spp. on the ability of strain HR92 to inhibit
327 *R. solanacearum* was analyzed by examining the biomass of *R. solanacearum*. All
328 treatments were performed with four replicates.

329 **Effect of strain HR92 on the ability of *Pseudarthrobacter* spp. to inhibit *R.***
330 ***solanacearum***

331 This experiment followed a three-step workflow similarly to the previous inhibition
332 assays. Initially, 2 μL of strain HR92 suspension (OD_{600} = 0.5) were incubated with 198
333 μL of NB medium at 30 °C with agitation at 170 rpm for 48 h, and the supernatant
334 (**supernatant d-1**) was collected after centrifugation. Next, 2 μL of *Pseudarthrobacter*
335 strains (strain P265 or P397) suspension (OD_{600} = 0.5) was incubated with 178 μL of
336 NB medium and 20 μL of **supernatant d-1** under similar conditions for 48 h, followed
337 by centrifugation to collect the supernatant (**supernatant d-2**). Finally, 2 μL of *R.*
338 *solanacearum* suspension (OD_{600} = 0.5) was incubated with 178 μL of NB medium
339 and 20 μL of **supernatant d-2** at 30 °C with agitation at 170 rpm for 48 h. We set
340 treatment without **supernatant d-2** (the same volume sterile water instead) as
341 control. Bacterial growth (OD_{600}) was measured using a SpectraMax M5
342 spectrophotometer (Molecular Devices, Sunnyvale, CA, USA). The effect of strain

343 HR92 on the ability of *Pseudarthrobacter* spp. to inhibit *R. solanacearum* was
344 analyzed by examining the biomass of *R. solanacearum*. All treatments were
345 performed with four replicates.

346 **RNA extraction and RNA-seq**

347 Total RNA was extracted from the bacterial cells using TRIzol® Reagent according the
348 manufacturer's instructions (Invitrogen, CA, USA). Then RNA quality was determined
349 using 2100 Bioanalyser (Agilent, CA, USA) and quantified using the ND-2000
350 (NanoDrop Technologies, DE, USA). RNA-seq strand-specific libraries were prepared
351 following TruSeq RNA sample preparation Kit from Illumina (San Diego, CA), using
352 5μg of total RNA. Shortly, rRNA removal by RiboZero rRNA removal kit (Epicenter,
353 Wisconsin, USA), fragmented using fragmentation buffer cDNA synthesis, end repair,
354 A-base addition and ligation of the Illumina-indexed adaptors were performed
355 according to Illumina's protocol. Libraries were then size selected for cDNA target
356 fragments of 200–300 bp on 2% Low Range Ultra Agarose followed by PCR amplified
357 using Phusion DNA polymerase (New England Biolabs, Massachusetts, USA) for 15
358 PCR cycles. After quantified by TBS380, paired-end libraries were sequenced by
359 Illumina NovaSeq 6000 sequencing (2 × 150bp, Shanghai BIOZERON Co., Ltd).
360 The raw paired end reads were trimmed and quality controlled by Trimmomatic with
361 parameters (SLIDINGWINDOW:4:15 MINLEN:75) (version 0.36
362 http://www.usadellab.org/cms/uploads/supplementary/Trimmomatic). Then clean
363 reads were separately aligned to reference genome with orientation mode using
364 Rockhopper (http://cs.wellesley.edu/~btjaden/Rockhopper/) software. Rockhopper
365 was a comprehensive and user-friendly system for computational analysis of
366 bacterial RNA-seq data. As input, Rockhopper takes RNA sequencing reads generated
367 by high-throughput sequencing technology. This software was used to calculate gene
368 expression levels with default parameters.

369 **Differential expression analysis and functional enrichment**

370 To identify differential expression genes (DEGs) between the two different samples,
371 the expression level for each transcript was calculated using the fragments per
372 kilobase of read per million mapped reads (RPKM) method. edgeR (51) was used for

373 differential expression analysis. The DEGs between two samples were selected using
374 the following criteria: the logarithmic of fold change was greater than 2 and the false
375 discovery rate (FDR) should be less than 0.05. To understand the functions of the
376 differential expressed genes, Gene Ontology (GO) functional enrichment and Kyoto
377 Encyclopedia and Genomes (KEGG) pathway analysis were carried out by Goatools
378 (52) and KOBAS (53) respectively. DEGs were significantly enriched in GO terms and
379 metabolic pathways when their Bonferroni-corrected P-value was less than 0.05.

380 **Effect of 3-methyl-1-butanol on the growth of pathogen *R. solanacearum***

381 In order to investigate the effect of key microbial metabolite on pathogen growth, we
382 used standard chemical compound of 3-methyl-1-butanol and *R. solanacearum* to
383 conduct a plate confrontation assay. The experiment was conducted using divided
384 Petri dishes, with a 1 cm diameter filter paper was placed on one side and NA
385 medium on the other. 3-methyl-1-butanol at concentrations ranging from 100%
386 purity to dilutions in dimethyl sulfoxide (DMSO) were applied to the filter paper (20
387 μl per dish). 5 μl of *R. solanacearum* (OD_{600} = 0.5) was inoculated onto the NB
388 medium, and plates were incubated at 30 ℃ for 48 h. After incubation, 1 ml of sterile
389 water was used to wash the bacterial colonies, and then 50 μl of the bacterial
390 suspension was diluted to 200 μl for OD_{600} measurements using a SpectraMax M5
391 spectrophotometer (Molecular Devices, Sunnyvale, CA, USA). DMSO was used as a
392 blank control. All treatments were performed with three replicates.

393 **Data analysis and statistics**

394 All data analyses were performed using R version 4.3.1. Microbiome community
395 diversity was calculated as ASVs. Changes in community composition were assessed
396 with a principal component analysis (PCA) by using the R package "microceo" v1.9.0
397 (54), function adonis in R package "vegan" v2.6.4 (55) was conducted to evaluate the
398 significant difference in community structure across the different treatments. The
399 "ONE_Tukey_HSD2" function was uesd to compare the differences between different
400 treatments. The "LorMe" v1.1.0 package (56) in the laboratory was employed to
401 construct microbial co-occurrence networks. The "ComplexHeatmap" v1.10.2
402 package (57) was utilized to depict the heatmap of bacterial resource utilization

403 ability.

404

405 # Results

406 **Effect of inulin on promoting pathogen suppression of *L. sphaericus* HR92**

407 To identify potential specific resource, we screened 13 water-soluble sugars based on
408 the criterion that they should not directly promote pathogen growth while
409 supporting the proliferation and antagonistic activity of beneficial bacteria. Initial in
410 vitro assays revealed that, except for allulose, none of the tested water-soluble
411 sugars significantly affected the growth of *R. solanacearum* ($F_{13,28}$ = 8.48, p < 0.001;
412 Fig. S2), indicating minimal risk of inadvertently stimulating pathogen development.
413 We next assessed the effects of these 12 sugars on the beneficial strain *L. sphaericus*
414 HR92 and its ability to inhibit *R. solanacearum*. Most sugars enhanced strain HR92
415 growth and strengthened its antagonistic activity, with inulin exhibiting the most
416 pronounced effect. Specifically, inulin significantly promoted HR92 growth ($F_{8,18}$ =
417 11.60, p < 0.001; Fig. S3A), with a maximum increase of 14.8%, and markedly
418 improved its inhibitory effect against *R. solanacearum*, achieving the highest
419 inhibition rate of 27.8% ($F_{8,18}$ = 10.74, p < 0.001; Fig. S3B). Given its dual benefits,
420 inulin was selected for subsequent experiments (Fig. S1).

421 In order to further verify effect of inulin on enhancing pathogen suppression of strain
422 HR92, we conducted a greenhouse experiment. Inoculation of strain HR92
423 significantly reduce disease index of tomato plants, and inulin addition strengthened
424 the disease suppression of strain HR92 with a dose effect ($F_{3,12}$ = 45.34, p < 0.05, Fig.
425 1A). The lowest disease index was observed in the treatment with 0.3% inulin and
426 strain HR92, which reduced by a 70% reduction compared to the control (CK, Fig. 1B).
427 Similarly, the *R. solanacearum* density in the rhizosphere of treatment with 0.3%
428 inulin and strain HR92 was the lowest ($F_{3,12}$ = 46.95, p < 0.05, Fig. 1B). Interestingly,
429 though 0.1% inulin increased the abundance of strain HR92 in the rhizosphere,
430 higher inulin concentration inulin (0.3%) did not further bring strain HR92 to a higher
431 density ($F_{3,12}$ = 13.223, p < 0.05, Fig. 1C). Additionally, we tested effect of inulin

concentration on the growth of strain HR92. Consistent with the in planta findings, 0.1% inulin significantly increased the growth of strain HR92, while 0.3% showed no significant improvement ($F_{3,8}$ = 14.51, $p < 0.05$, Fig. S4). These findings indicate the effect of inulin on improving pathogen suppression of strain HR92, but not in a dose dependent way.

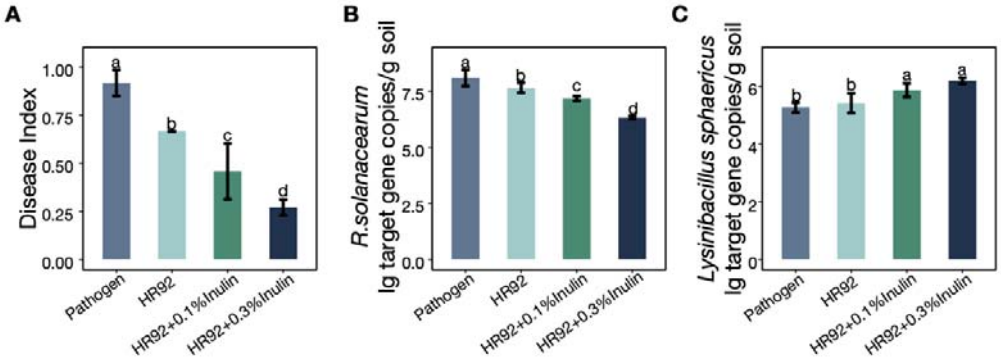

Fig. 1 **Effects of inulin on enhancing pathogen suppression by strain HR92 in tomato bacterial wilt**.

(A) Tomato disease index under different treatments (N = 4). (B) Absolute abundance of *R. solanacearum* in the tomato rhizosphere under different treatments, quantified by qPCR using species-specific primers (one-way ANOVA with correction by Tukey's HSD test; N = 4). (C) Absolute abundance of HR92 in the tomato rhizosphere under different treatments, quantified by qPCR using species-specific primers (one-way ANOVA with correction by Tukey's HSD test; N = 4). Different letters in the bar graph indicate significant differences ($p < 0.05$).

Strain HR92 and inulin alter the bacterial community of the tomato rhizosphere

16S rRNA gene amplicon sequencing was conducted to reveal the differences in the rhizosphere bacterial community among the four treatments. There were no significant differences in the Simpson and Shannon diversity indices between the control group and the HR92 or HR92+0.1% inulin treatment groups. However, the addition of 0.3% inulin with strain HR92 significantly decreased both the Simpson and Shannon indices of the tomato rhizosphere bacterial community (Shannon: $F_{3,12}$ = 9.26, p = 0.02, Fig 2A; Simpson $F_{3,12}$ = 3.36, p = 0.04, Fig 2B).

Principal coordinates analysis (PCoA) revealed significant differences in the bacterial community composition among the four treatments. Inoculating HR92 can alter the tomato rhizosphere microbial community, and the addition of inulin can further modify the microbial community structure, with distinct differences observed

459 between the 0.1% and 0.3% inulin treatments, being especially clear along the PCo1,
460 which explained 29.1% of the total variation in bacterial community composition
461 (PERMANOVA, R^2 = 0.460, p = 0.001, Fig. 2C).
462 Further analysis of the relative abundance of bacteria in different treatments
463 revealed that bacteria amplicon sequence variants (ASVs) primarily belonged to 10
464 phyla, including *Proteobacteria*, *Acidobacteria*, *Bacteroidetes*, *Verrucomicrobia*,
465 *Chloroflexi*, *Actinobacteria*, *Patescibacteria*, *Gemmatimonadetes*, *Myxococcota*, and
466 *Firmicutes*. Although the composition of dominant bacterial phyla was similar across
467 treatments, the relative abundance of certain dominant phyla differed significantly.
468 Specifically, the phylum *Patescibacteria* was significantly enriched in the treatment
469 with 0.3% inulin and strain HR92 (Fig. 2D).

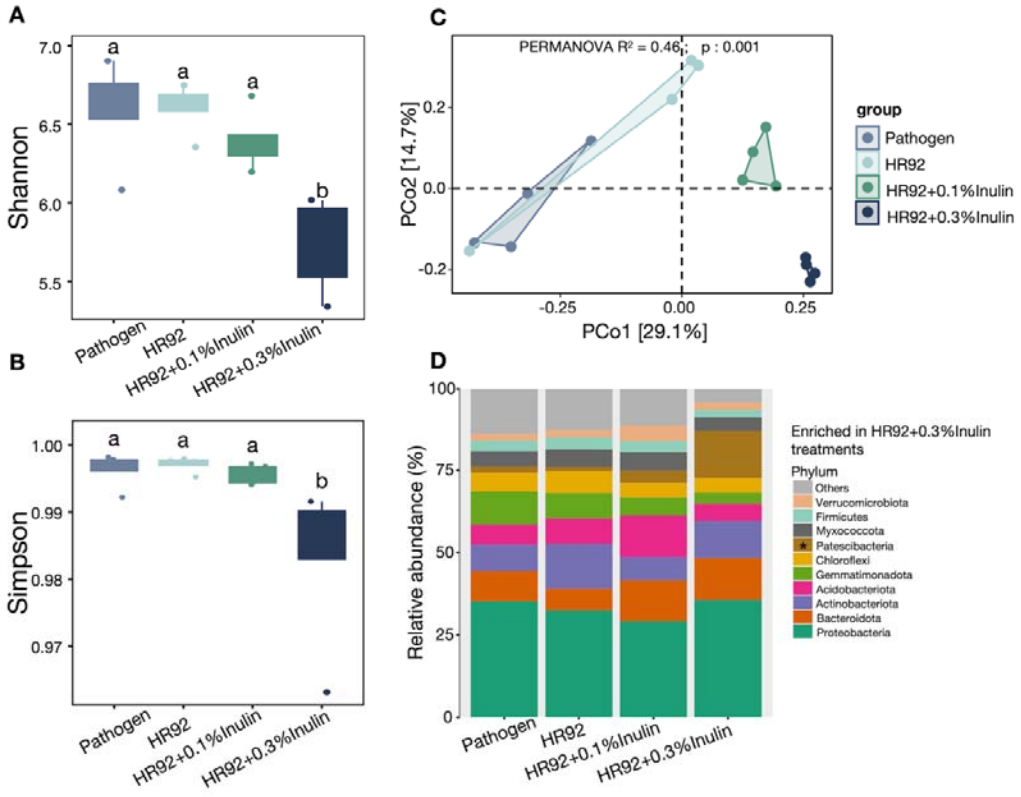

470

471 Fig. 2 **Microbial community analysis under different treatments.** (A) Alpha diversity analysis of
472 the rhizosphere microbiome across treatments using the Shannon index. (B) Alpha diversity
473 analysis using the Simpson index. (C) PCoA of the rhizosphere soil microbiota under each
474 treatment. (D) Relative abundance of the top 10 most abundant phyla in the rhizosphere soil
475 across treatments. The asterisk indicates phyla enriched specifically in the HR92+0.3% inulin
476 treatment compared to the other treatments. Different letters above the boxes of each
477 compartment indicate a significant difference at $p < 0.05$ (one-way ANOVA with correction by

478 Tukey's HSD test).

479 **Inulin stimulates native soil resident microbes to assist strain HR92 in resisting *R.***
480 ***solanacearum* invasion**

481 Following the application of 0.3% inulin in combination with HR92, the colonization
482 of HR92 in the rhizosphere did not significantly increase (Fig. 1C). However, the
483 disease index of tomatoes and the population of rhizosphere *R. solanacearum*
484 further decreased (Fig. 1A, B). We hypothesize that, beyond its direct effect on HR92,
485 the 0.3% inulin may enrich certain native soil resident microbes that contribute to
486 pathogen suppression. Subsequently, 21 genera significantly enriched in the
487 treatment with 0.3% inulin were identified, defining them as potential key taxa (Table
488 S1, $p < 0.05$).

489 Further analysis of co-occurrence networks and distribution patterns of dominant
490 genera across the four treatments identified key taxa. Notably, among the top ten
491 nodes in the co-occurrence network based on betweenness centrality, two ASVs,
492 ASV2 (*Pseudarthrobacter*) and ASV201 (*Agromyces*), were recognized as potential
493 keystone bacteria (Fig. 3A). The relative abundance of ASV2 was significantly
494 correlated with inulin concentration, with its abundance further increasing under the
495 0.3% inulin treatment, whereas ASV201 was enriched exclusively in the 0.3% inulin
496 treatment (ASV2: $F_{3,12} = 13.16$, $p < 0.001$; ASV201: $F_{3,12} = 19.18$, $p < 0.001$, Fig. 3B).
497 Both ASV2 (R = -0.82, $p < 0.05$) and ASV201 (R = -0.81, $p < 0.05$) exhibited significant
498 negative correlations with the abundance of *R. solanacearum*, and
499 *Pseudarthrobacter* ($R = -0.77$, $p < 0.05$) and *Agromyces* ($R = -0.75$, $p < 0.05$) also
500 demonstrated significant negative correlations with the abundance of *R.*
501 *solanacearum* (Fig. S5A, B). Thus, *Pseudarthrobacter* and *Agromyces* are considered
502 potential key taxa that interact synergistically with HR92 to confer disease resistance.

503 Additionally, microorganisms enriched under the 0.3% inulin treatment were
504 predominantly concentrated within modules 2 and 3 of the co-occurrence network,
505 both of which were significantly negatively correlated with pathogen abundance
506 (module 2: $R = -0.69$, $p < 0.05$; module 3: $R = -0.82$, $p < 0.05$; Fig. S5C, D), suggesting
507 their crucial roles in disease suppression.

508 Tax4Fun functional prediction indicated that *Pseudarthrobacter* is primarily

associated with secondary metabolite synthesis, basic metabolism, and isoflavonoid biosynthesis, suggesting that *Pseudarthrobacter* may mediate disease resistance via these pathways (Fig. S6). Given its significant association with disease suppression and its tenfold higher abundance compared to *Agromyces* in the tomato rhizosphere, *Pseudarthrobacter* likely plays a more prominent role in mediating rhizosphere interactions. Therefore, subsequent validation experiments focused on *Pseudarthrobacter*.

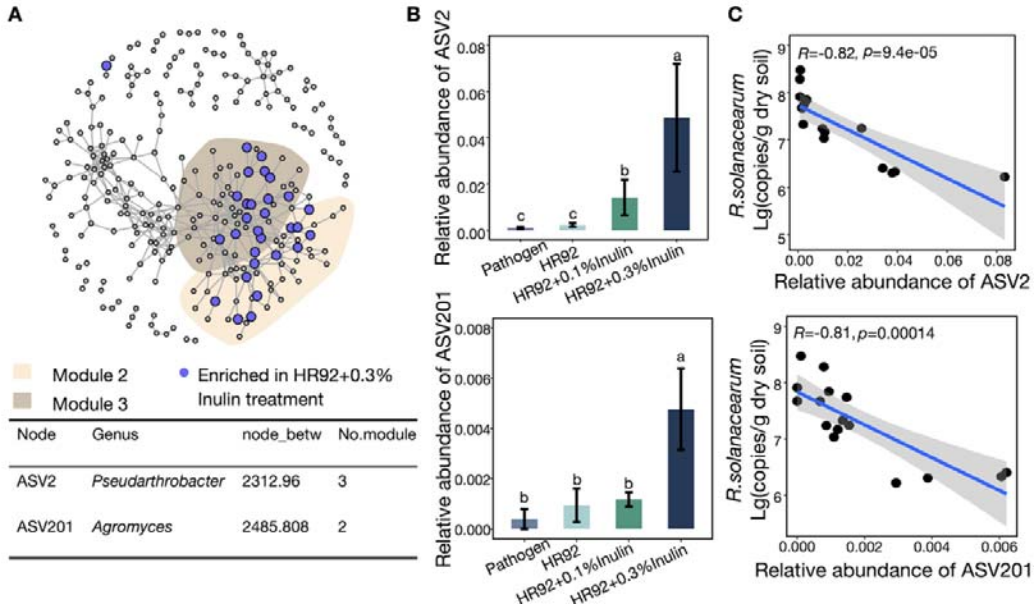

Fig. 3 **Co-occurrence network analysis.** (A) The co-occurrence network at the ASV level, where the purple nodes represent ASVs enriched under high-concentration inulin treatment. Key nodes and their properties are detailed below the network graph. (B) Relative abundance of ASV2 and ASV201 in the rhizosphere microbial communities across four treatments (N = 4; one-way ANOVA with correction by Tukey's HSD test). (C) Linear regression between the relative abundance of ASV2 and ASV201 and the population of *R.solanacearum* in the tomato rhizosphere ($p < 0.05$). Different letters in the graph indicate significant differences ($p < 0.05$).

***Pseudarthrobacter* strains in cooperative interaction with HR92 to suppress *R. solanacearum* invasion**

To evaluate the effect of *Pseudarthrobacter* on disease suppression and explore its underlying mechanisms, we isolated 50 culturable bacterial strains from soil treated with 0.3% inulin. Among these, strains P265 and P397 were identified as members of the genus *Pseudarthrobacter*. These two strains were used to investigate the specific mechanisms involved. First, we examined the effect of inulin on the growth of the

531 two bacterial strains and found that inulin significantly promoted the growth of strain
532 P265 and P397 (strain P265: t-test: $t_{6.32}$ = -2.82, p = 0.029; strain P397: t-test: $t_{8.67}$ =
533 -6.42, p < 0.001; Fig. 4A), indicating that these bacteria effectively utilized inulin as a
534 resource. We subsequently assessed the potential of strain P265 and P397 to inhibit
535 pathogenic activity. In vitro assays demonstrated that the supernatants from P265
536 and P397 did not directly inhibit *R. solanacearum* (strain P265: $F_{2,11}$ = 0.69, p = 0.5;
537 strain P397: $F_{2,11}$ = 1.15, p = 0.5, Fig. S8). However, under co-culture conditions, both
538 P265 and P397 inhibited the growth of *R. solanacearum*, the inhibition rate of P265
539 was 41%, and that of P397 was 41.4%, with the addition of inulin showing no
540 significant influence on this inhibitory effect (strain P265: $F_{2,9}$ = 130.13, p < 0.001;
541 strain P397: $F_{2,9}$ = 56.58, p < 0.001; Fig. 4B). These observations suggest that the
542 inhibitory mechanism may involve nutrient competition between these strains and *R.*
543 *solanacearum*.
544 To explore nutrient competition we examined the utilization of 74 different
545 rhizosphere carbon sources by P265, P397, and *R. solanacearum*. The results
546 indicated that P265 and P397 utilized a broader range of resources compared to *R.*
547 *solanacearum* (Table 2, p < 0.05). The overlap in resource utilization between P265
548 and *R. solanacearum* was 0.94, and between P397 and *R. solanacearum* was 0.91 (Fig.
549 4C), indicating potential competition for carbon resources between
550 *Pseudarthrobacter* strains and *R. solanacearum*.
551 Additionally, the supernatant from the co-culture of strain HR92 with P265 or P397
552 showed an enhanced inhibitory effect against *R. solanacearum* (strain P265: $F_{3,12}$ =
553 19.18, p < 0.001; strain P397: $F_{3,12}$ = 22.35, p < 0.001; Fig. 4D). We hypothesized that
554 either strain HR92 induced antibacterial activity in strains P265 and P397 or that
555 these strains augmented strain HR92's antibacterial function. To test this hypothesis,
556 first, we fed the supernatant of strain HR92 to P265 and P397. Subsequently, we fed
557 the supernatants of P265 and P397 to *R. solanacearum* and found that the growth of
558 *R. solanacearum* was not affected (strain P265: $F_{2,18}$ = 1.834, p = 0.18; strain P397:
559 $F_{2,18}$ = 1.55, p = 0.24, Fig. S9). This indicates that strain HR92 was unable to confer the
560 ability to antagonize *R. solanacearum* to P265 or P397. Conversely, we fed the

561 supernatant of strain P265 or P397 to strain HR92 and found that the supernatant of
562 strain HR92 had a stronger ability to inhibit *R. solanacearum*, with enhancements of
563 12% and 6.6%, respectively (strain P265: $F_{2,9}$ = 46.23, p < 0.001; strain P397: $F_{2,9}$ =
564 33.306, p < 0.001; Fig. 4E). In pot experiments, consistent with the in vitro findings,
565 strains P265 and P397 enhanced the ability of strain HR92 to mitigate tomato
566 bacterial wilt. Notably, the combined treatment of strain HR92, *Pseudarthrobacter*
567 strains, and inulin provided the best protection against tomato bacterial wilt, with a
568 disease index of 0.3375 (P265) and 0.35 (P397), achieving control efficiencies of 61.9%
569 (P265) and 60.5% (P397) ($F_{6,21}$ = 87.21, p < 0.001, Fig. 4F).

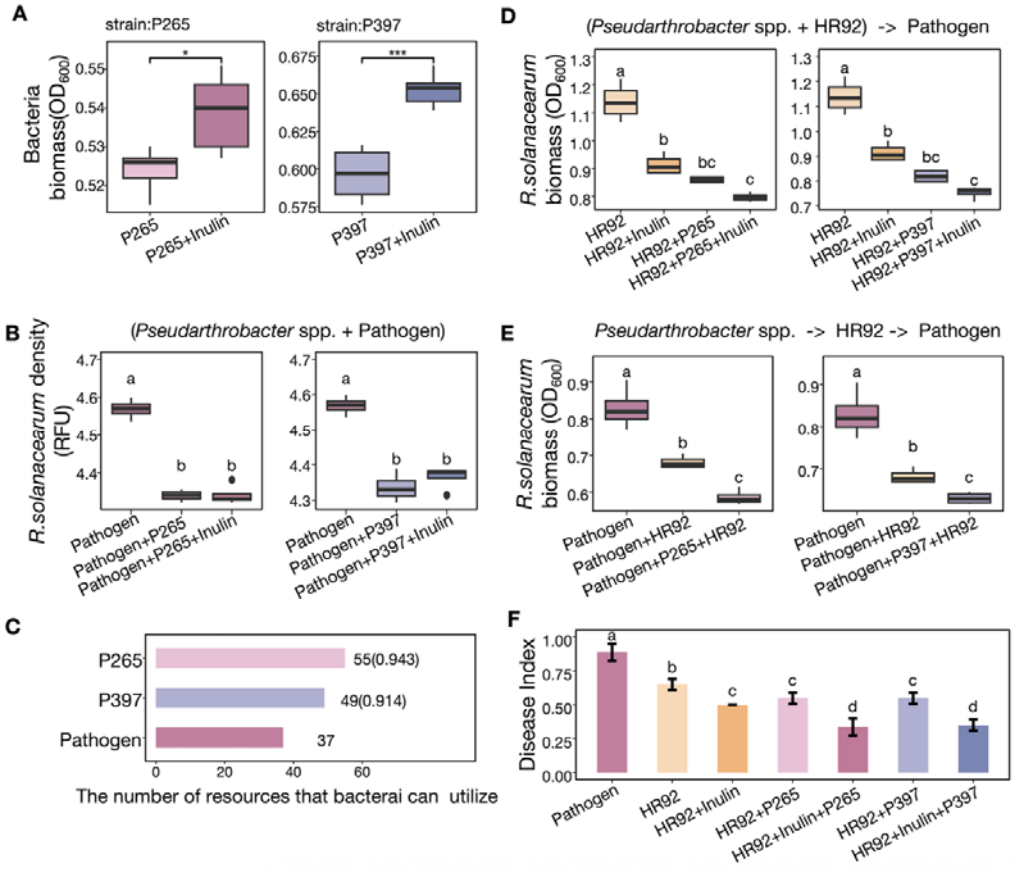

570

571 Fig. 4 **Investigation of the antibacterial effects of *Pseudarthrobacter* spp. and its influence on**
572 **the antibacterial activity of HR92.** (A) Effect of inulin on the growth of *Pseudarthrobacter*
573 *siccitolerans* (P265) and *Pseudarthrobacter oxydans* (P397). Asterisk means p < 0.05 and three
574 asterisks means p < 0.001 under student's t test (N = 4). (B) Inhibition of *R. solanacearum* by
575 strains P265 and P397 under co-culture conditions with and without the addition of inulin. (C)
576 Resource utilization overlap between strain P265/P397 and *R. solanacearum*, indicating the
577 potential nutritional competition. (D) Enhanced antibacterial activity of the supernatant after
578 co-culture of strain HR92 with strains P265 and P397. The arrows at the top of the box plot

represent the feeding procedure. Specifically, they indicate feeding the pathogen with the supernatant from co-cultures of strain P267 or P397 and strain HR92. (E) Increased antibacterial activity of HR92 after being cultured with the supernatants from strains P265/P397. The arrows at the top of the box plot represent the feeding procedure. Specifically, they indicate feeding strain HR92 with the supernatant from strain P267 or P397, followed by feeding the pathogen with the supernatant from strain HR92. (F) Pot experiments showing enhanced tomato disease resistance when HR92, *Pseudarthrobacter* strains, and inulin were applied together. Different letters in the graph indicate significant differences ($p < 0.05$).

***Pseudarthrobacter* strains and inulin enhance cyclic lipopeptide surfactin and 3-methyl-1-butanol production by HR92**

Transcriptomic analysis was conducted to elucidate the individual and combined effects of inulin and *Pseudarthrobacter* strains on strain HR92. Inulin upregulated genes involved in flagellar assembly, bacterial chemotaxis, fatty acid biosynthesis, and siderophore biosynthesis in strain HR92, indicating that inulin enhances the motility of HR92 in the rhizosphere, thereby increasing its colonization quantity(Fig. S10). Strains P265 and P397 collectively influenced genes expression in strain HR92, with significant differential expression observed in genes related to the synthesis of 4-aminobutyrate, methyl-accepting, butanediol and bacitracin, all of which are associated with strain HR92's antimicrobial activity (Fig. S11). Bacitracin is a broad-spectrum antibiotic known for its antimicrobial properties. Furthermore, the combined action of *Pseudarthrobacter* strains and inulin enhanced the synthesis of amino acids such as valine and leucine in HR92 (Fig. S12, Fig. S13). Subsequent Weighted Gene Co-expression Network Analysis (WGCNA) identified three gene modules in strain HR92 that were linked to its antimicrobial activity (Fig. S14). Within the black and pink modules, two genes highly correlated with the modules and exhibiting the highest correlation with strain HR92's antimicrobial effect were identified: LYS2002816 and LYS2001501. These genes were associated with butanediol and NAD(P)H, both of which exhibited a significant positive correlation with strain HR92's antimicrobial capability (LYS2002816: $R = 0.79$, $p < 0.05$, LYS2001501: $R = 0.73$, $p < 0.05$, Fig. S15). The abundance of these genes was highest in strain P265 or P397, HR92, and inulin treatment (LYS2002816: $F_{5,12} = 2.9$, $p < 0.05$, Figure 5A; LYS2001501: $F_{5,12} = 5.8$, $p < 0.05$, Figure 5B). Literature review indicated that butanediol contributes to the synthesis of the volatile antimicrobial compound

612 3-methyl-1-butanol in strain HR92, whereas fatty acids, NAD(P)H, valine, and leucine
613 are involved in the synthesis of the cyclic lipopeptide surfactin (Fig. 5C, D), ultimately
614 enhancing strain HR92's ability to inhibit *R. solanacearum*.
615 To further elucidate the role of 3-methyl-1-butanol, we tested its effect on *R.*
616 *solanacearum* growth. Our results showed that 50% and 100% concentrations of
617 3-methyl-1-butanol could inhibit the growth of *R. solanacearum*, with 50%
618 concentration resulting in a 16.4% inhibition rate and 100% concentration achieving
619 a 40% inhibition rate ($F_{4,10}$ = 6.839, $p < 0.05$, Fig. S16).

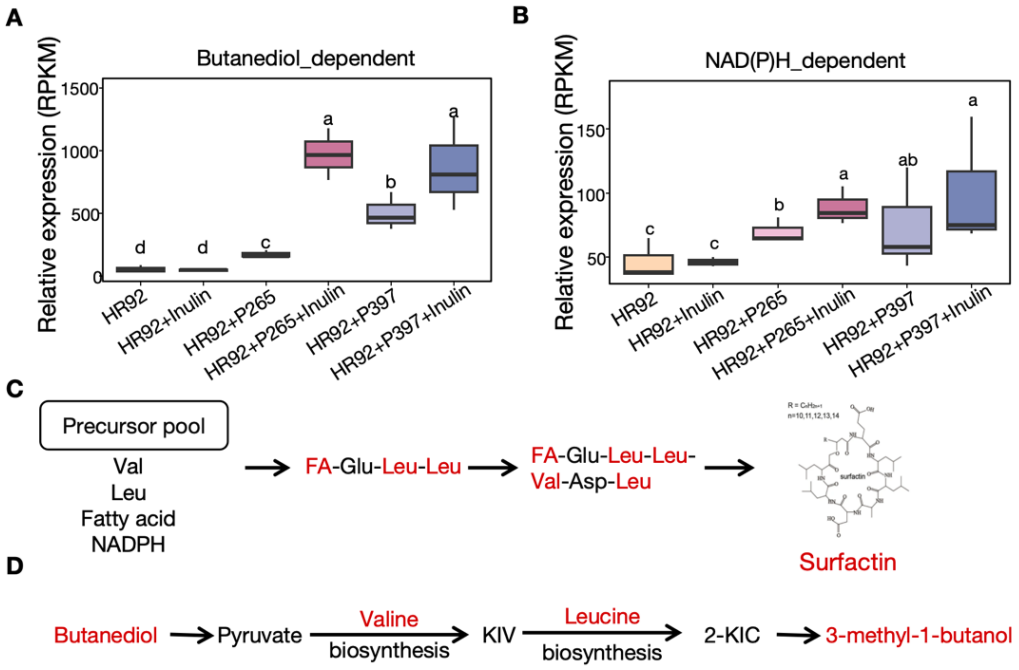

620
621 Fig. 5 **Synergistic enhancement of HR92 antibacterial capability by *Pseudarthrobacter* spp. and**
622 **inulin.** (A) Expression levels of HR92 genes associated with butanediol synthesis across six
623 treatments, quantified by RPKM tables. (B) Expression levels of HR92 genes involved in NAD(P)H
624 synthesis across six treatments, quantified by RPKM tables. Different letters in the graph indicate
625 significant differences (Duncan's multiple range test). (C) Schematic diagram illustrating the
626 involvement of fatty acids, NAD(P)H, valine, and leucine in the biosynthesis of the cyclic
627 lipopeptide surfactin. (D) Schematic diagram showing the pathway through which butanediol is
628 converted to 3-methyl-1-butanol via pyruvate, valine biosynthesis, and leucine biosynthesis
629 pathways. Red font highlights the pathways or genes influenced by the synergistic action of
630 *Pseudarthrobacter* spp. and inulin.

631 ## Discussion

632 There is growing interest in harnessing beneficial bacteria for plant disease
633 biocontrol, yet strategies to maxmize their effectiveness remain insufficiently

634 explored. Here, our study emphasizes the important role of inulin in promoting the
635 growth and pathogen-suppressing capabilities of the beneficial strain HR92, along
636 with its synergistic interactions with native soil microbes to manage *R. solanacearum*
637 infections in tomatoes. We also investigated whether increased inulin
638 concentrations could further improve the biocontrol efficacy of strain HR92. Both *in*
639 *vitro* and *in vivo* experiments demonstrated that inulin positively influenced bacterial
640 colonization and biocontrol efficiency. In general, higher inulin concentrations
641 selectively enriched *Pseudarthrobacter* species in the soil, which acted synergistically
642 with strain HR92 to enhance biocontrol outcomes.
643 Inulin promoted strain HR92 growth and augmented its pathogen-suppressing ability.
644 Initially, we observed a threefold increase in strain HR92 population in the tomato
645 rhizosphere upon inulin treatment. This finding is consistent with previous studies
646 showing that inulin selectively stimulates the growth of beneficial bacteria, such as
647 *Bifidobacterium*, *Lactobacillus*, and *Bacteroides,* while inhibiting potential pathogens
648 (58). Additionally, inulin has been shown to increase the production of lactic acid,
649 acetic acid, and other volatile compounds by probiotic strains, indicating a positive
650 synergistic interaction between inulin and beneficial microbes (59). These findings
651 support our results that inulin, as a prebiotic, promotes the growth of beneficial
652 bacteria. We further discovered that the disease severity index for tomatoes treated
653 with both inulin and strain HR92 decreased by 31.2% compared to those treated with
654 strain HR92 alone. Previous research has demonstrated that strain HR92 could
655 effectively control *R. solanacearum* (19), suggesting a direct impact of strain HR92 on
656 the *R. solanacearum*. This can be interpreted as the biocontrol efficacy of beneficial
657 bacteria being closely related to their abundance in the rhizosphere (60), and that
658 plant-derived carbon sources could enhance the metabolic activity of specific
659 beneficial bacteria, thereby improving their disease resistance (61, 62). Furthermore,
660 we observed that increasing the inulin concentration from 0.1% to 0.3% did not
661 further promote the growth of strain HR92, which may be due to strain HR92 already
662 obtaining sufficient nutrients at the 0.1% concentration. The optimal inulin

663 concentration for promoting strain HR92 growth under complex environmental
664 conditions remains to be further investigated.
665 Inulin and its varying concentrations significantly influenced rhizosphere microbial
666 diversity and community structure. While a low inulin concentration (0.1%) had no
667 significant effect on the Simpson and Shannon diversity indices, a higher
668 concentration (0.3%) reduced these indices. This can be explained by higher
669 concentrations of inulin potentially altering community structure by selectively
670 enriching certain functional bacteria, thereby reducing the relative abundance of
671 other bacterial groups. Our findings revealed distinct differences in bacterial
672 community composition between the two inulin concentrations treatments. Previous
673 studies have indicated that the concentration of exogenous carbon sources in soil has
674 a significant selective effect on native microbial communities (40, 63). Taken together,
675 different concentrations of inulin can regulate the interactions and structure of
676 native microbial communities, maintaining higher diversity at lower concentrations
677 while promoting the enrichment of specific functional bacteria at higher
678 concentrations. Since a higher concentration of inulin further reduced disease
679 severity and the abundance of *R. solanacearum* in the rhizosphere, without altering
680 the abundance of strain HR92 in the rhizosphere. Therefore, we hypothesize that,
681 beyond directly benefiting strain HR92, a 0.3% inulin concentration may also enrich
682 certain native soil microbes that aid in suppressing pathogens. In fact, in the
683 co-occurrence network analysis, *Pseudarthrobacter* and *Agromyces* were significantly
684 enriched under high inulin concentration treatment and identified as key network
685 hubs, rowten showing a significant negative correlation with the pathogen. This
686 suggests that they may support strain HR92's pathogen suppression function through
687 competition or antagonistic interactions. Interestingly, previous studies have
688 indicated that *Pseudarthrobacter* is adept at collaborating with other beneficial
689 bacteria to perform better ecological functions (64). On the other hand, strains
690 belonging to the genus *Pseudarthrobacter* are known as copiotrophic root colonizers
691 (65, 66) and have been proposed as a key members of the root microbiome (67). In

692 summary, the present study highlights the importance of the synergistic interaction
693 between inulin, *Pseudarthrobacter* and HR92 in managing *Ralstonia solanacearum*.
694 Our study also demonstrates that the combined effects of inulin and
695 *Pseudarthrobacter* strains significantly enhance the antibacterial activity of HR92
696 against *R. solanacearum*, primarily through the upregulation of genes related to the
697 synthesis of key metabolites, such as surfactin and 3-methyl-1-butanol. The
698 inhibitory effects of these metabolites on pathogens have been well-documented.
699 The cyclic lipopeptide surfactin, a polypeptide compound composed of fatty acids
700 and amino acids, exhibits notable antimicrobial, antiviral, and plant
701 stress-resistance-promoting activities, playing a particularly prominent role in disease
702 defense (68). Transcriptomic analysis in this study revealed that inulin and
703 *Pseudarthrobacter* strains promoted the synthesis of surfactin by upregulating
704 metabolic pathways related to fatty acids and amino acids, such as valine and leucine.
705 Furthermore, 3-methyl-1-butanol, as a volatile antimicrobial compound, has shown
706 high efficacy in inhibiting various pathogens. Its mode of action involves binding to
707 microbial cell membranes, inserting into the bilayer structure, and altering
708 membrane permeability, which destabilizes the membrane, causes leakage of cellular
709 contents such as ions and ATP, and ultimately leads to cell death, effectively inhibiting
710 pathogen growth (69, 70). Our co-expression network analysis of HR92 genes
711 indicated that the butanediol and NADPH metabolic pathways are closely associated
712 with the antibacterial potential of HR92, possibly by promoting the synthesis of
713 3-methyl-1-butanol. Further experimental validation confirmed that high
714 concentrations of 3-methyl-1-butanol exhibit strong inhibitory effects on *R.*
715 *solanacearum*, which is consistent with other studies on volatile organic compounds
716 (VOCs) as disease suppressants (71). In summary, these results suggest that the
717 synergistic effects of inulin and *Pseudarthrobacter* can significantly enhance HR92's
718 ability to suppress *R. solanacearum* by promoting the synthesis of key antibacterial
719 metabolites.
720 In conclusion, our study demonstrates that the inulin significantly enhances strain
721 HR92 colonization, chemotaxis, fatty acid metabolism, and siderophore production in

722 tomato roots. The addition of 0.3% inulin had a greater impact than 0.1%, notably
723 enriching *Pseudarthrobacter* species within the rhizosphere. These species promoted
724 the synthesis of butanediol and bacitracin in strain HR92, thereby enhancing its
725 antimicrobial capabilities. Furthermore, *Pseudarthrobacter* spp. competed with *R.*
726 *solanacearum* for root-associated resources, reducing the abundance of pathogenic
727 bacteria via nutrient competition. The combined effects of *Pseudarthrobacter* spp.
728 and inulin further upregulated strain HR92's valine and leucine metabolic pathways.
729 Valine, leucine, fatty acids, and NAD(P)H are essential precursors for *L. sphaericus* to
730 synthesize the antimicrobial cyclic lipopeptide surfactin. Additionally, butanediol is
731 converted into the antimicrobial VOC 3-methyl-1-butanol through valine and leucine
732 metabolic pathways. Thus, the cooperative interaction between *Pseudarthrobacter*
733 spp. and inulin enhanced strain HR92's ability to inhibit *R. solanacearum*, ultimately
734 reducing the incidence of tomato disease. This research provides valuable insights
735 into the synergistic interactions between exogenous additives and beneficial
736 microbes, offering a foundation for developing advanced, targeted formulations for
737 sustainable and effective disease management (Fig 6).

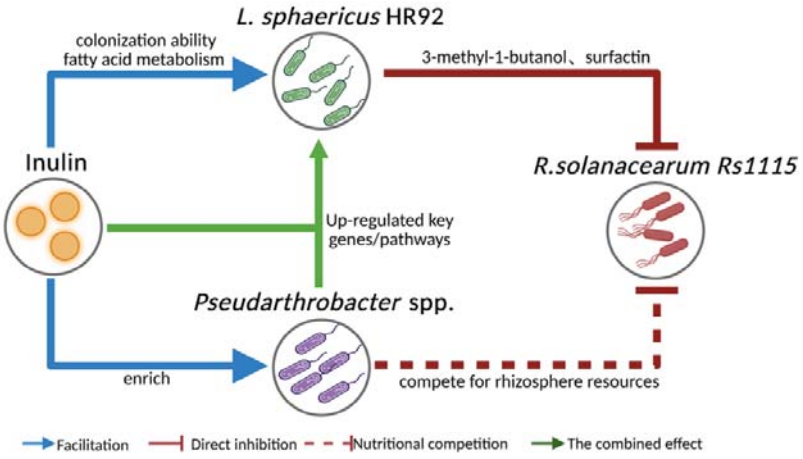

738

739 Fig. 6 Pathways by which inulin enhances HR92's disease-resistance mechanisms.
740 Blue arrows indicate promotion effects, red solid lines indicate direct inhibition effects, red
741 dashed lines indicate inhibition of pathogen growth through nutrient competition.

742 **Data availability**

743 All metagenomics reads are publicly available in the SRA database under the
744 accession number PRJNA1198698.

Acknowledgments

This work was financially supported by the National Key Technology R&D Program of China (2023YFD1701505), the National Key Research and Development Program of China (2024YFC3406003), Guangxi Science and Technology Program (GuiKe AA24010003), the National Nature Science Foundation of China (42477125, 42090060, 42325704), the Natural Science Foundation of Jiangsu Province (BK20230988), the Technology Innovation Special Fund of Jiangsu Province for Carbon Dioxide Emission Peaking and Carbon Neutrality (BE2022423).

Conflict of Interest

The authors declare no competing interests.

758 ## References

759 1. Liu J, Yao Q, Li Y, Zhang W, Mi G, Chen X, Yu Z, Wang G. 2019. Continuous cropping of
760 soybean alters the bulk and rhizospheric soil fungal communities in a Mollisol of Northeast
761 PR China. Land Degrad Dev 30:1725–1738.
762 2. Zheng GD, Shi LB, Wu HY, Peng DL. 2012. Nematode communities in continuous
763 tomato-cropping field soil infested by root-knot nematodes. Acta Agriculturae Scandinavica,
764 Section B - Soil & Plant Science 62:216–223.
765 3. Tsiafouli MA, Thébault E, Sgardelis SP, De Ruiter PC, Van Der Putten WH, Birkhofer K,
766 Hemerik L, De Vries FT, Bardgett RD, Brady MV, Bjornlund L, Jørgensen HB, Christensen S,
767 Hertefeldt TD, Hotes S, Gera Hol WH, Frouz J, Liiri M, Mortimer SR, Setälä H, Tzanopoulos J,
768 Uteseny K, Pižl V, Stary J, Wolters V, Hedlund K. 2015. Intensive agriculture reduces soil
769 biodiversity across Europe. Global Change Biology 21:973–985.
770 4. Raaijmakers JM, Mazzola M. 2016. Soil immune responses. Science 352:1392–1393.
771 5. Delgado-Baquerizo M, Guerra CA, Cano-Díaz C, Egidi E, Wang J-T, Eisenhauer N, Singh BK,
772 Maestre FT. 2020. The proportion of soil-borne pathogens increases with warming at the
773 global scale. Nat Clim Chang 10:550–554.
774 6. Andreote FD, Pereira E Silva MDC. 2017. Microbial communities associated with plants:
775 learning from nature to apply it in agriculture. Current Opinion in Microbiology 37:29–34.
776 7. Yuan W, Ruan S, Qi G, Wang R, Zhao X. 2022. Plant growth-promoting and antibacterial
777 activities of cultivable bacteria alive in tobacco field against *Ralstonia solanacearum*.
778 Environmental Microbiology 24:1411–1429.
779 8. Sanguin H, Sarniguet A, Gazengel K, Moënne-Loccoz Y, Grundmann GL. 2009. Rhizosphere
780 bacterial communities associated with disease suppressiveness stages of take-all decline in
781 wheat monoculture. New Phytologist 184:694–707.
782 9. Zhou X, Wang J, Liu F, Liang J, Zhao P, Tsui CKM, Cai L. 2023. Author Correction:
783 Cross-kingdom synthetic microbiota supports tomato suppression of Fusarium wilt disease.
784 Nat Commun 14:6755.
785 10. Li M, Pommier T, Yin Y, Wang J, Gu S, Jousset A, Keuskamp J, Wang H, Wei Z, Xu Y, Shen Q,
786 Kowalchuk GA. 2022. Indirect reduction of Ralstonia solanacearum via pathogen helper
787 inhibition. ISME J 16:868–875.
788 11. Wu B, Wang X, Yang L, Yang H, Zeng H, Qiu Y, Wang C, Yu J, Li J, Xu D, He Z, Chen S. 2016.
789 Effects of Bacillus amyloliquefaciens ZM9 on bacterial wilt and rhizosphere microbial
790 communities of tobacco. Applied Soil Ecology 103:1–12.
791 12. Wang N, Ding J, Chen Y, Zhu Y, Zhang L, Wei Y, Li J, Xu T, Ding G. 2023. *Bacillus velezensis*
792 BER1 enriched *Flavobacterium daejeonense* -like bacterium in the rhizosphere of tomato
793 against bacterial wilt. FEMS Microbiology Ecology 99:fiad054.
794 13. Wang X, Li G-H, Zou C-G, Ji X-L, Liu T, Zhao P-J, Liang L-M, Xu J-P, An Z-Q, Zheng X, Qin Y-K,
795 Tian M-Q, Xu Y-Y, Ma Y-C, Yu Z-F, Huang X-W, Liu S-Q, Niu X-M, Yang J-K, Huang Y, Zhang K-Q.
796 2014. Bacteria can mobilize nematode-trapping fungi to kill nematodes. Nat Commun
797 5:5776.
798 14. Wei Z, Yang T, Friman V-P, Xu Y, Shen Q, Jousset A. 2015. Trophic network architecture of
799 root-associated bacterial communities determines pathogen invasion and plant health. Nat
800 Commun 6:8413.

801 15. Hase S, Shimizu A, Nakaho K, Takenaka S, Takahashi H. 2006. Induction of transient ethylene
802 and reduction in severity of tomato bacterial wilt by *Pythium oligandrum*. Plant Pathology
803 55:537–543.
804 16. Sakthivel K, Manigundan K, Gautam RK, Singh PK, Balamurugan A, Kumar A, Sharma SK.
805 2023. Microbe-enriched farm yard manure (MFYM) approach for the suppression of
806 Ralstonia solanacearum Yabuuchi (Smith) inciting bacterial wilt disease in eggplant (Solanum
807 melongena L.). Plant Soil 491:303–315.
808 17. Jamal QMS, Ahmad V. 2022. Lysinibacilli: A Biological Factories Intended for Bio-Insecticidal,
809 Bio-Control, and Bioremediation Activities. JoF 8:1288.
810 18. Shabanamol S, Thampi M, Sajana P, Varghese S, Karthika S, George TK, Jisha MS. 2021.
811 Characterization of the major antifungal extrolite from rice endophyte Lysinibacillus
812 sphaericus against Rhizoctonia solani. Arch Microbiol 203:2605–2613.
813 19. Huang J, Wei Z, Tan S, Mei X, Yin S, Shen Q, Xu Y. 2013. The rhizosphere soil of diseased
814 tomato plants as a source for novel microorganisms to control bacterial wilt. Applied Soil
815 Ecology 72:79–84.
816 20. Yoon, M.Y. Lysinibacillus sphaericus TC1 Strain and Method for Controlling Plant Diseases
817 Using the Same. Patent Application No. KR20140051676A, 2 May 2014.
818 21. Akintayo SO, Treinen C, Vahidinasab M, Pfannstiel J, Bertsche U, Fadahunsi I, Oellig C,
819 Granvogl M, Henkel M, Lilge L, Hausmann R. 2022. Exploration of surfactin production by
820 newly isolated Bacillus and Lysinibacillus strains from food-related sources. Letters in
821 Applied Microbiology 75:378–387.
822 22. Zhi Y, Wu Q, Xu Y. 2017. Genome and transcriptome analysis of surfactin biosynthesis in
823 Bacillus amyloliquefaciens MT45. Sci Rep 7:40976.
824 23. Sakthivel K, Manigundan K, Gautam RK, Singh PK, Yogeshwari, Subramani T, Sharma SK,
825 Khande R. 2018. Bioefficacy of antimicrobial peptide biosynthesis-gene-linked antagonistic
826 Lysinibacillus sphaericus strains for management of bacterial plant diseases in Andaman and
827 Nicobar Islands, India. JEB 39:517–521.
828 24. Wei Z, Huang J, Yang T, Jousset A, Xu Y, Shen Q, Friman V-P. 2017. Seasonal variation in the
829 biocontrol efficiency of bacterial wilt is driven by temperature-mediated changes in bacterial
830 competitive interactions. J Appl Ecol 54:1440–1448.
831 25. El-Hassan SA, Gowen SR. 2006. Formulation and Delivery of the Bacterial Antagonist *Bacillus*
832 *subtilis* for Management of Lentil Vascular Wilt Caused by *Fusarium oxysporum* f. sp. *lentis*.
833 Journal of Phytopathology 154:148–155.
834 26. Albright MBN, Louca S, Winkler DE, Feeser KL, Haig S-J, Whiteson KL, Emerson JB, Dunbar J.
835 2022. Solutions in microbiome engineering: prioritizing barriers to organism establishment.
836 The ISME Journal 16:331–338.
837 27. Kaminsky LM, Trexler RV, Malik RJ, Hockett KL, Bell TH. 2019. The Inherent Conflicts in
838 Developing Soil Microbial Inoculants. Trends in Biotechnology 37:140–151.
839 28. El Fantroussi S, Agathos SN. 2005. Is bioaugmentation a feasible strategy for pollutant
840 removal and site remediation? Current Opinion in Microbiology 8:268–275.
841 29. Tao C, Li R, Xiong W, Shen Z, Liu S, Wang B, Ruan Y, Geisen S, Shen Q, Kowalchuk GA. 2020.
842 Bio-organic fertilizers stimulate indigenous soil Pseudomonas populations to enhance plant
843 disease suppression. Microbiome 8:137.
844 30. Gu Y, Hou Y, Huang D, Hao Z, Wang X, Wei Z, Jousset A, Tan S, Xu D, Shen Q, Xu Y, Friman V-P.

845 2017. Application of biochar reduces Ralstonia solanacearum infection via effects on
846 pathogen chemotaxis, swarming motility, and root exudate adsorption. Plant Soil
847 415:269–281.
848 31. Jin X, Rahman MKU, Ma C, Zheng X, Wu F, Zhou X. 2023. Silicon modification improves
849 biochar's ability to mitigate cadmium toxicity in tomato by enhancing root colonization of
850 plant-beneficial bacteria. Ecotoxicology and Environmental Safety 249:114407.
851 32. Wang X, Zhang Y, Xu W, Cheng J, Liu J, Pei W, Wang J, Chuang S. 2023. Amino acid fertilizer
852 strengthens its effect on crop yield and quality by recruiting beneficial rhizosphere microbes.
853 J Sci Food Agric 103:5970–5980.
854 33. Hu Y, Li Y, Yang X, Li C, Wang L, Feng J, Chen S, Li X, Yang Y. 2021. Effects of integrated
855 biocontrol on bacterial wilt and rhizosphere bacterial community of tobacco. Sci Rep
856 11:2653.
857 34. Yuan S, Wang L, Wu K, Shi J, Wang M, Yang X, Shen Q, Shen B. 2014. Evaluation of
858 Bacillus-fortified organic fertilizer for controlling tobacco bacterial wilt in greenhouse and
859 field experiments. Applied Soil Ecology 75:86–94.
860 35. Matsuzaki C, Takagi H, Saiga S, Kinoshita Y, Yamaguchi M, Higashimura Y, Yamamoto K,
861 Yamaguchi M. 2024. Prebiotic effect of galacto- *N* -biose on the intestinal lactic acid bacteria
862 as enhancer of acetate production and hypothetical colonization. Appl Environ Microbiol
863 e01445-23.
864 36. Bertelsen RJ, Jensen ET, Ringel-Kulka T. 2016. Use of probiotics and prebiotics in infant
865 feeding. Best Practice & Research Clinical Gastroenterology 30:39–48.
866 37. Sánchez ÓJ, Ospina DA, Montoya S. 2017. Compost supplementation with nutrients and
867 microorganisms in composting process. Waste Management 69:136–153.
868 38. Xiong Q, Liu D, Zhang H, Dong X, Zhang G, Liu Y, Zhang R. 2020. Quorum sensing signal
869 autoinducer-2 promotes root colonization of Bacillus velezensis SQR9 by affecting biofilm
870 formation and motility. Appl Microbiol Biotechnol 104:7177–7185.
871 39. Xu Z, Zhang H, Sun X, Liu Y, Yan W, Xun W, Shen Q, Zhang R. 2019. *Bacillus velezensis* Wall
872 Teichoic Acids Are Required for Biofilm Formation and Root Colonization. Appl Environ
873 Microbiol 85:e02116-18.
874 40. Wen T, Xie P, Liu H, Liu T, Zhao M, Yang S, Niu G, Hale L, Singh BK, Kowalchuk GA, Shen Q,
875 Yuan J. 2023. Tapping the rhizosphere metabolites for the prebiotic control of soil-borne
876 bacterial wilt disease. Nat Commun 14:4497.
877 41. Xu Z, Xie J, Zhang H, Wang D, Shen Q, Zhang R. 2019. Enhanced Control of Plant Wilt Disease
878 by a Xylose-Inducible *degQ* Gene Engineered into *Bacillus velezensis* Strain SQR9XYQ.
879 Phytopathology® 109:36–43.
880 42. Kim L, Mogk A, Schumann W. 1996. A xylose-inducible Bacillus subtilis integration vector and
881 its application. Gene 181:71–76.
882 43. Wei Z, Yang X, Yin S, Shen Q, Ran W, Xu Y. 2011. Efficacy of Bacillus-fortified organic fertiliser
883 in controlling bacterial wilt of tomato in the field. Applied Soil Ecology 48:152–159.
884 44. Guo J-H, Qi H-Y, Guo Y-H, Ge H-L, Gong L-Y, Zhang L-X, Sun P-H. 2004. Biocontrol of tomato
885 wilt by plant growth-promoting rhizobacteria. Biological Control 29:66–72.
886 45. Cardenas E, Wu W-M, Leigh MB, Carley J, Carroll S, Gentry T, Luo J, Watson D, Gu B,
887 Ginder-Vogel M, Kitanidis PK, Jardine PM, Zhou J, Criddle CS, Marsh TL, Tiedje JM. 2010.
888 Significant Association between Sulfate-Reducing Bacteria and Uranium-Reducing Microbial

889 Communities as Revealed by a Combined Massively Parallel Sequencing-Indicator Species
890 Approach. Appl Environ Microbiol 76:6778–6786.
891 46. Callahan BJ, McMurdie PJ, Rosen MJ, Han AW, Johnson AJA, Holmes SP. 2016. DADA2:
892 High-resolution sample inference from Illumina amplicon data. Nat Methods 13:581–583.
893 47. Caporaso JG, Kuczynski J, Stombaugh J, Bittinger K, Bushman FD, Costello EK, Fierer N, Peña
894 AG, Goodrich JK, Gordon JI, Huttley GA, Kelley ST, Knights D, Koenig JE, Ley RE, Lozupone CA,
895 McDonald D, Muegge BD, Pirrung M, Reeder J, Sevinsky JR, Turnbaugh PJ, Walters WA,
896 Widmann J, Yatsunenko T, Zaneveld J, Knight R. 2010. QIIME allows analysis of
897 high-throughput community sequencing data. Nat Methods 7:335–336.
898 48. Schönfeld J, Heuer H, Van Elsas JD, K. Smalla. 2003. Specific and Sensitive Detection of
899 *Ralstoniasolanacearum* in Soil on the Basis of PCR Amplification of *fliC* Fragments. Appl
900 Environ Microbiol 69:7248–7256.
901 49. Eden PA, Schmidt TM, Blakemore RP, Pace NR. 1991. Phylogenetic Analysis of Aquaspirillum
902 magnetotacticum Using Polymerase Chain Reaction-Amplified 16S rRNA-Specific DNA.
903 International Journal of Systematic Bacteriology 41:324–325.
904 50. Scheublin TR, Sanders IR, Keel C, Van Der Meer JR. 2010. Characterisation of microbial
905 communities colonising the hyphal surfaces of arbuscular mycorrhizal fungi. The ISME
906 Journal 4:752–763.
907 51. Robinson MD, McCarthy DJ, Smyth GK. 2010. edgeR: a Bioconductor package for
908 differential expression analysis of digital gene expression data. Bioinformatics 26:139–140.
909 52. Klopfenstein DV, Zhang L, Pedersen BS, Ramírez F, Warwick Vesztrocy A, Naldi A, Mungall CJ,
910 Yunes JM, Botvinnik O, Weigel M, Dampier W, Dessimoz C, Flick P, Tang H. 2018. GOATOOLS:
911 A Python library for Gene Ontology analyses. Sci Rep 8:10872.
912 53. Wu J, Mao X, Cai T, Luo J, Wei L. 2006. KOBAS server: a web-based platform for automated
913 annotation and pathway identification. Nucleic Acids Research 34:W720–W724.
914 54. Liu C, Cui Y, Li X, Yao M. 2021. *microeco*: an R package for data mining in microbial
915 community ecology. FEMS Microbiology Ecology 97:fiaa255.
916 55. Dixon P. 2003. VEGAN, a package of R functions for community ecology. J Vegetation Science
917 14:927–930.
918 56. Wang N, Zhang Y, Jiang G. 2024. LorMe: Lightening One-Code Resolving Microbial Ecology
919 Solution.
920 57. Gu Z, Eils R, Schlesner M. 2016. Complex heatmaps reveal patterns and correlations in
921 multidimensional genomic data. Bioinformatics 32:2847–2849.
922 58. Havenaar R, Bonnin-Marol S, Van Dokkum W, Petitet S, Schaafsma G. 1999. Inulin:
923 Fermentation and microbial ecology in the intestinal tract. Food Reviews International
924 15:109–120.
925 59. Oliveira RPDS, Perego P, De Oliveira MN, Converti A. 2012. Growth, organic acids profile and
926 sugar metabolism of Bifidobacterium lactis in co-culture with Streptococcus thermophilus:
927 The inulin effect. Food Research International 48:21–27.
928 60. Wang NR, Wiesmann CL, Melnyk RA, Hossain SS, Chi M-H, Martens K, Craven K, Haney CH.
929 2022. Commensal Pseudomonas fluorescens Strains Protect *Arabidopsis* from Closely
930 Related Pseudomonas Pathogens in a Colonization-Dependent Manner. mBio 13:e02892-21.
931 61. Stringlis IA, Yu K, Feussner K, De Jonge R, Van Bentum S, Van Verk MC, Berendsen RL, Bakker
932 PAHM, Feussner I, Pieterse CMJ. 2018. MYB72-dependent coumarin exudation shapes root

933 microbiome assembly to promote plant health. Proc Natl Acad Sci USA 115.
934 62. Feng H, Fu R, Luo J, Hou X, Gao K, Su L, Xu Y, Miao Y, Liu Y, Xu Z, Zhang N, Shen Q, Xun W,
935 Zhang R. 2023. Listening to plant's Esperanto via root exudates: reprogramming the
936 functional expression of plant growth-promoting rhizobacteria. New Phytologist
937 239:2307–2319.
938 63. Ling N, Raza W, Ma J, Huang Q, Shen Q. 2011. Identification and role of organic acids in
939 watermelon root exudates for recruiting Paenibacillus polymyxa SQR-21 in the rhizosphere.
940 European Journal of Soil Biology 47:374–379.
941 64. Naloka K, Kuntaveesuk A, Muangchinda C, Chavanich S, Viyakarn V, Chen B, Pinyakong O.
942 2024. Pseudomonas and Pseudarthrobacter are the key players in synergistic phenanthrene
943 biodegradation at low temperatures. Sci Rep 14:11976.
944 65. Samal S, Singh D, Upadhyay RS, Lokesh Babu P, Geat N. 2024. Hydrolytic genes of
945 antagonistic rhizobacteria strains on Fusarium udum causing wilt disease in pigeonpea. J
946 Plant Pathol https://doi.org/10.1007/s42161-024-01641-z.
947 66. Ghasemi Z, Ghaderian SM, Rodríguez-Garrido B, Prieto-Fernández Á, Kidd PS. 2018. Plant
948 species-specificity and effects of bioinoculants and fertilization on plant performance for
949 nickel phytomining. Plant Soil 425:265–285.
950 67. Adamo I, Acin-Albiac M, Röttjers S, De Prado DR, Benito BM, Zamora J, Godara R,
951 García-Jiménez B, Jiang-Rempel P, Cline LC, Acedo A. 2024. Short impact on soil microbiome
952 of a Bacillus amyloliquefaciens QST713 based product that correlates with higher potato
953 yield across USA. Front Plant Sci 15:1332840.
954 68. Laird M, Piccoli D, Weselowski B, McDowell T, Renaud J, MacDonald J, Yuan Z-C. 2020.
955 Surfactin-producing Bacillus velezensis 1B-23 and Bacillus sp. 1D-12 protect tomato against
956 bacterial canker caused by Clavibacter michiganensis subsp. michiganensis. J Plant Pathol
957 102:451–458.
958 69. Huang R, Li GQ, Zhang J, Yang L, Che HJ, Jiang DH, Huang HC. 2011. Control of Postharvest
959 Botrytis Fruit Rot of Strawberry by Volatile Organic Compounds of *Candida intermedia*.
960 Phytopathology 101:859–869.
961 70. Zhao X, Zhou J, Tian R, Liu Y. 2022. Microbial volatile organic compounds: Antifungal
962 mechanisms, applications, and challenges. Front Microbiol 13:922450.
963 71. Zhou X, Zhang J, Shi J, Khashi U Rahman M, Liu H, Wei Z, Wu F, Dini-Andreote F. 2024.
964 Volatile-mediated interspecific plant interaction promotes root colonization by beneficial
965 bacteria via induced shifts in root exudation. Microbiome 12:207.
966

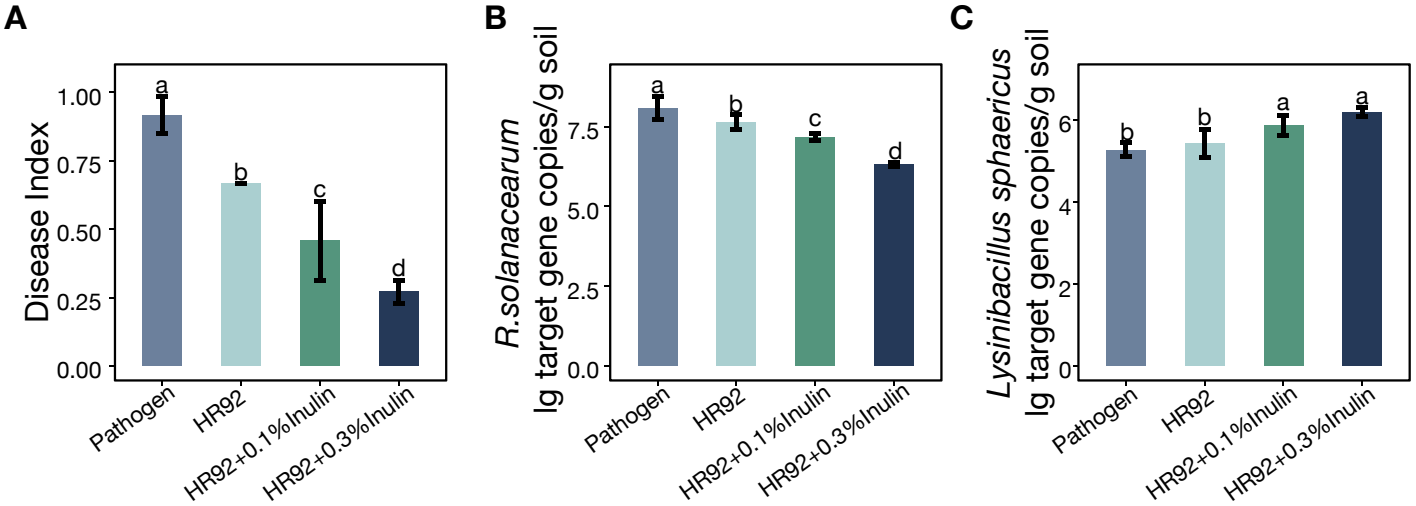
A
Disease Index
1.00
0.75
0.50
0.25
0.00
a
b
c
d
Pathogen
HR92
HR92+0.1%Inulin
HR92+0.3%Inulin
B
R.solanacearum
lg target gene copies/g soil
7.5
5.0
2.5
0.0
a
b
c
d
Pathogen
HR92
HR92+0.1%Inulin
HR92+0.3%Inulin
C
Lysinibacillus sphaericus
lg target gene copies/g soil
6
4
2
0
b
b
a
a
Pathogen
HR92
HR92+0.1%Inulin
HR92+0.3%Inulin

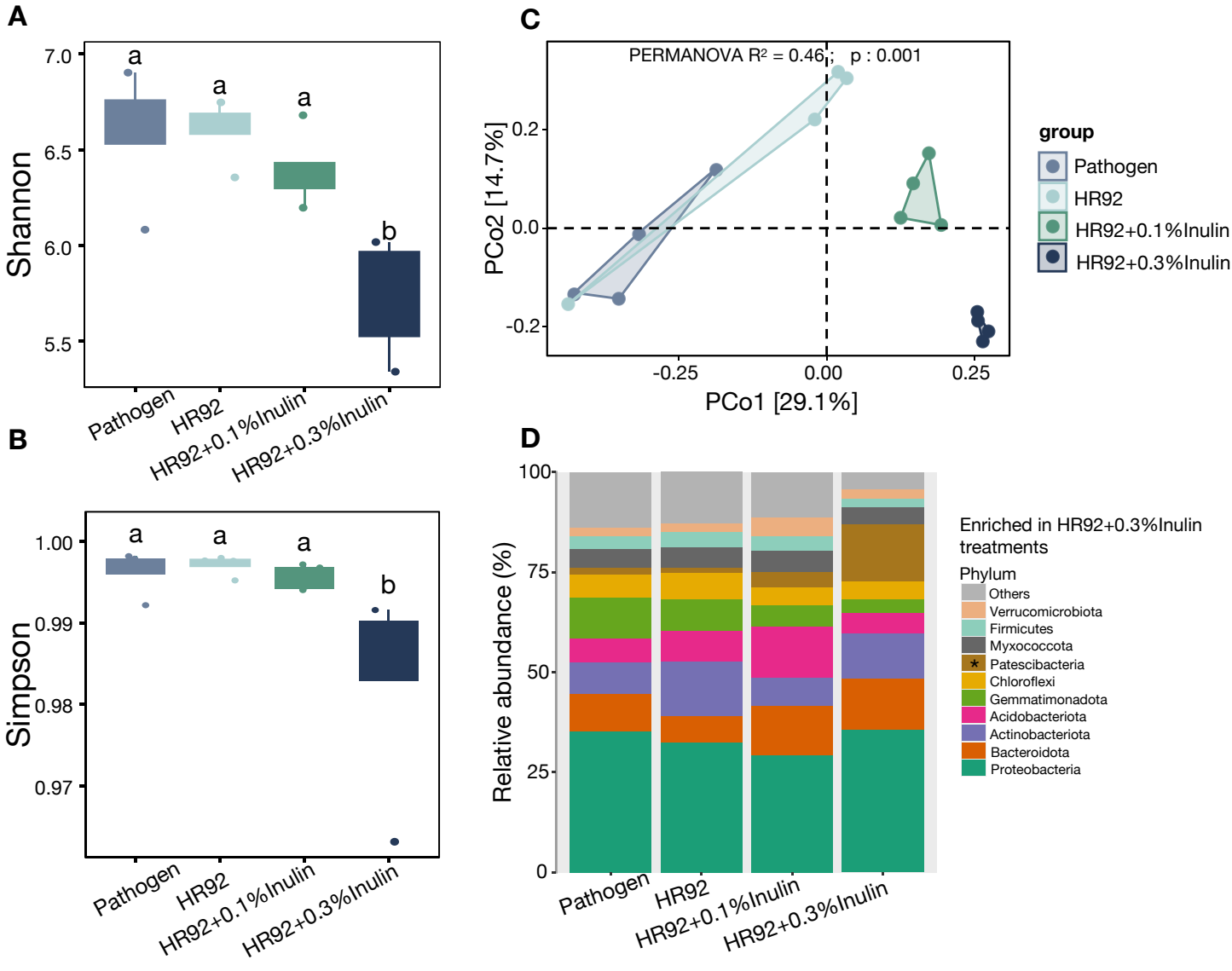
A
Shannon
7.0
6.5
6.0
5.5
a
a
a
b
Pathogen
HR92
HR92+0.1%Inulin
HR92+0.3%Inulin
B
Simpson
1.00
0.99
0.98
0.97
a
a
a
b
Pathogen
HR92
HR92+0.1%Inulin
HR92+0.3%Inulin
C
PERMANOVA R² = 0.46 ; p : 0.001
PCo2 [14.7%]
0.2
0.0
-0.2
-0.25
0.00
0.25
PCo1 [29.1%]
group
Pathogen
HR92
HR92+0.1%Inulin
HR92+0.3%Inulin
D
Relative abundance (%)
100
75
50
25
0
Pathogen
HR92
HR92+0.1%Inulin
HR92+0.3%Inulin
Enriched in HR92+0.3%Inulin treatments
Phylum
Others
Verrucomicrobiota
Firmicutes
Myxococcota
* Patescibacteria
Chloroflexi
Gemmatimonadota
Acidobacteriota
Actinobacteriota
Bacteroidota
Proteobacteria

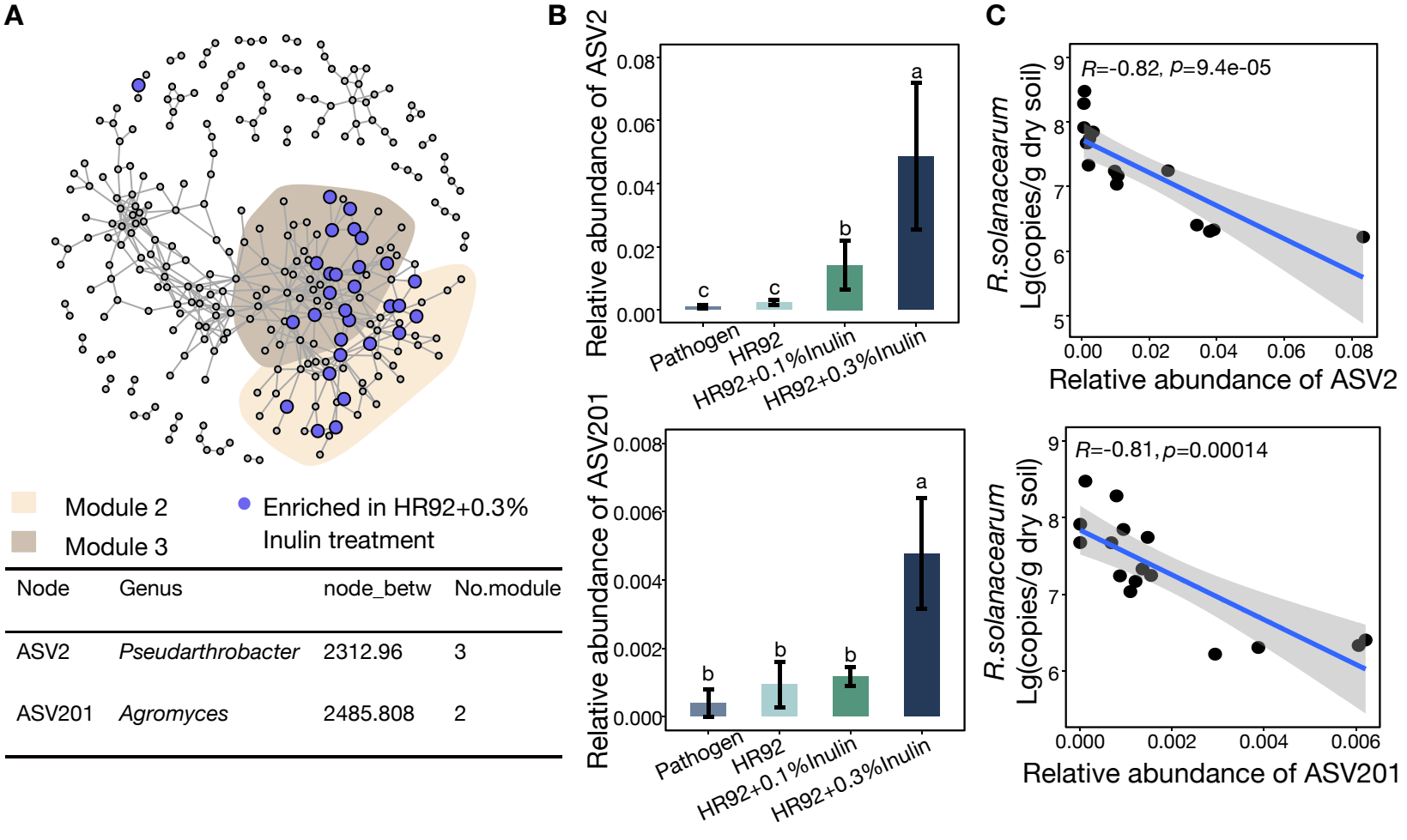

Node	Genus	node_betw	No.module
ASV2	*Pseudarthrobacter*	2312.96	3
ASV201	*Agromyces*	2485.808	2

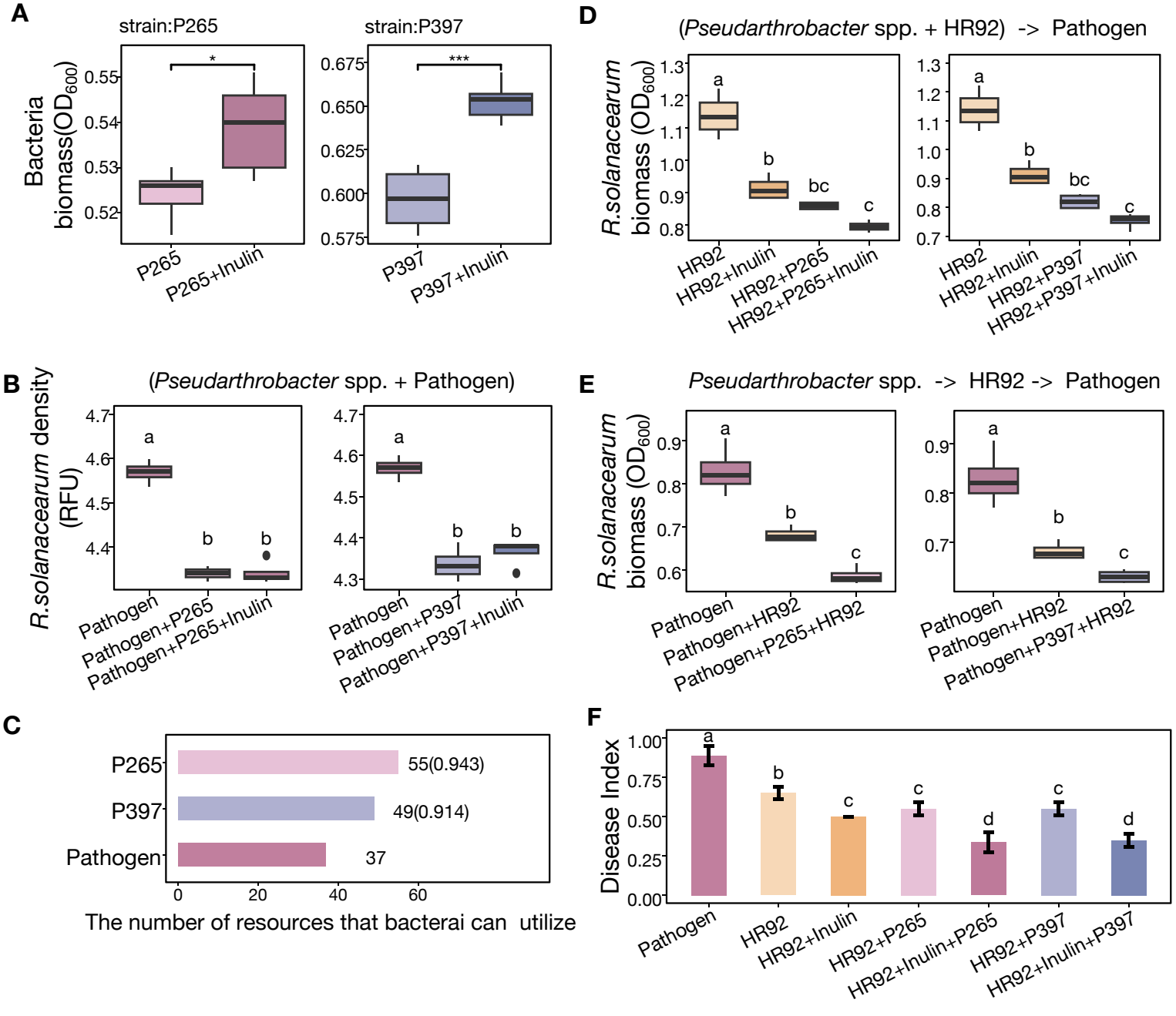
A
strain:P265
strain:P397
Bacteria biomass(OD600)
*
***
P265
P265+Inulin
P397
P397+Inulin
B
(Pseudarthrobacter spp. + Pathogen)
R.solanacearum density (RFU)
Pathogen
Pathogen+P265
Pathogen+P265+Inulin
Pathogen+P397
Pathogen+P397+Inulin
C
P265
P397
Pathogen
55(0.943)
49(0.914)
37
The number of resources that bacterai can utilize
D
(Pseudarthrobacter spp. + HR92) -> Pathogen
R.solanacearum biomass (OD600)
HR92
HR92+Inulin
HR92+P265
HR92+P265+Inulin
HR92+P397
HR92+P397+Inulin
E
Pseudarthrobacter spp. -> HR92 -> Pathogen
Pathogen+HR92
Pathogen+P265+HR92
Pathogen+P397+HR92
F
Disease Index
Pathogen
HR92
HR92+Inulin
HR92+P265
HR92+Inulin+P265
HR92+P397
HR92+Inulin+P397

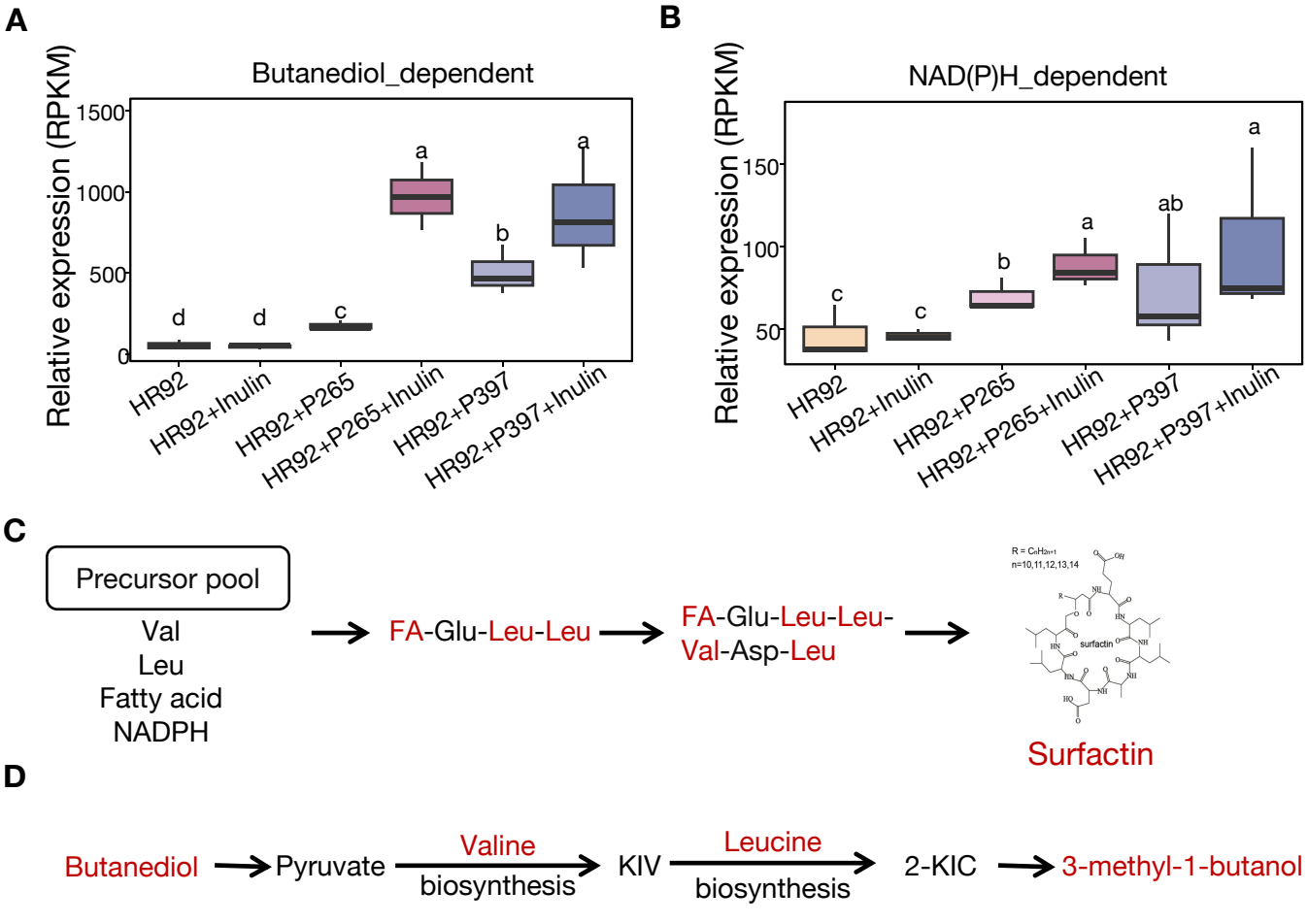
A
Butanediol_dependent
Relative expression (RPKM)
1500
1000
500
0
d
d
c
a
b
a
HR92
HR92+Inulin
HR92+P265
HR92+P265+Inulin
HR92+P397
HR92+P397+Inulin
B
NAD(P)H_dependent
Relative expression (RPKM)
150
100
50
c
c
b
a
ab
a
HR92
HR92+Inulin
HR92+P265
HR92+P265+Inulin
HR92+P397
HR92+P397+Inulin
C
Precursor pool
Val
Leu
Fatty acid
NADPH
FA-Glu-Leu-Leu
FA-Glu-Leu-Leu-
Val-Asp-Leu
Surfactin
D
Butanediol
Pyruvate
Valine
biosynthesis
KIV
Leucine
biosynthesis
2-KIC
3-methyl-1-butanol

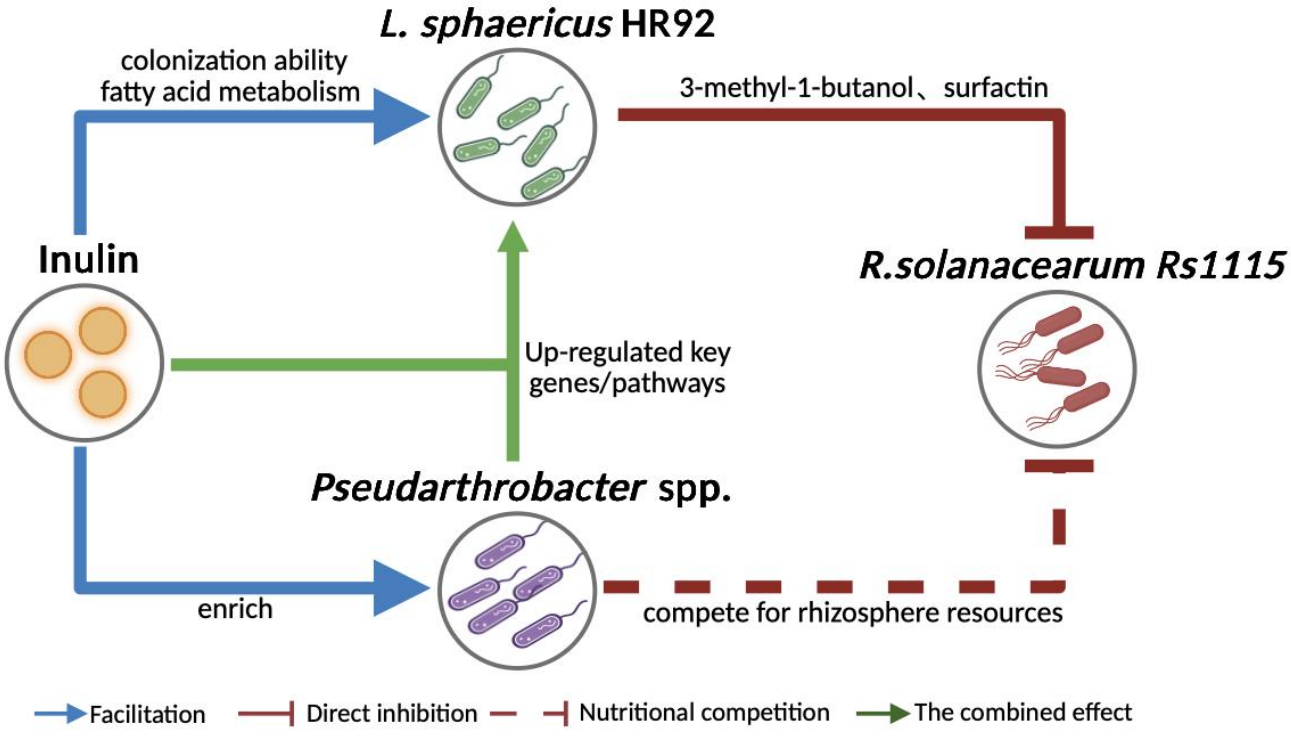
L. sphaericus HR92
colonization ability
fatty acid metabolism
3-methyl-1-butanol、surfactin
Inulin
R.solanacearum Rs1115
Up-regulated key
genes/pathways
Pseudarthrobacter spp.
enrich
compete for rhizosphere resources
Facilitation
Direct inhibition
Nutritional competition
The combined effect